A BIOFILM MODEL THAT AVOIDS

A TRAGEDY OF THE COMMONS

by

Seth Aaron Dayutis

A thesis submitted in partial fulfillment
of the requirements for the degree

of

Master of Science

in

Mathematics

MONTANA STATE UNIVERSITY
Bozeman, Montana

April, 2021

DEDICATION

This thesis is dedicated to my grandfather who passed away during my first semester of graduate school. He earned his Master's degree in English from Boston College. I am happy to have the opportunity to earn my Master's degree in Mathematics and follow his legacy of education.

ACKNOWLEDGEMENTS

First and foremost, I want to thank Jack Dockery for his support throughout this thesis. His advice, assistance and patience in dealing with my constant questions about implementing boundary conditions were crucial in finishing this project. His passion for mathematics was inspiring to me and I appreciate having him as my advisor. I would also like to thank my committee members, Scott McCalla and Tomas Gedeon for their willingness to undertake this journey with me. Finally, I want to thank all my friends and family members who offered words of support along the way, none of this would have been possible without their encouragement.

TABLE OF CONTENTS

LIST OF TABLES

Table Page

LIST OF FIGURES

LIST OF FIGURES – CONTINUED

Figure Page

LIST OF ALGORITHMS

ABSTRACT

The study of competition between multiple species is of great significance in biology. Competitive behavior is often observed to occur in biofilms and understanding cooperation between multiple species in a single biofilm is the center of much research. The species that grow in biofilms are frequently studied in chemostats, which have a rich history in mathematical modeling. In this thesis, a review of a mathematical chemostat model is presented in which a tragedy of the commons occurs. The chemostat model is then developed into a biofilm model to see if a tragedy occurs in a biofilm under similar conditions. The biofilm and chemostat model consist of two species, a cooperator and a cheater. The cooperator produces an enzyme that combines with a substrate to produce a nutrient. The nutrient is then consumed by the cooperator and cheater. The cooperator is at a disadvantage since it must allocate some of its nutrient uptake towards enzyme production. A one dimensional biofilm model is developed with reaction advection equations governing the behavior of the species and reaction-diffusion equations governing the behavior of the substrate, nutrient ,and enzyme. A set of numerical methods is then outlined on how to solve the system of equations. It is found that a tragedy of the commons is avoided in the biofilm and both species can persist when numerical simulations are run for a finite amount of time. It is then argued that the cooperative behavior exhibited by the two species is a stable equilibrium by approximating the steady state solutions. Further evidence is provided for the existence of a stable equilibrium by perturbing the system and finding that the perturbed system tends back to the equilibrium. Finally, the eigenvalues of the discretized linear system are computed and the results suggest that either the equilibrium is stable or moves away from the equilibrium slowly.

1

INTRODUCTION

The tragedy of the commons is a well-studied phenomenon in fields ranging from economics to biology. It is useful to use an analogy to make this concept more concrete. Hardin establishes the tragedy with the following analogy from his now-famous 1968 paper [7]. There is a pasture where all the herdsman in a village are allowed to graze their cattle. Naturally, the herdsman want to have both the healthiest and largest amount of cattle. So all the herdsman let their cattle graze on the land with no restraint. Eventually all of the food is depleted and the cattle end up dying off [7], because no one takes care of the land. The tragedy of the commons describes scenarios in which public goods are used by different individuals or groups, but no one actually owns the public goods. The idea is that since nobody owns the public goods, there is no incentive to maintain these goods. The eventual outcome of the tragedy of the commons is an overuse of public goods that ultimately leads to their destruction and all those that depend on the commons.

The tragedy of the commons is a story about competition. One place where competition is prevalent is in biology. Biologists are often interested in studying the competition between certain species. A particular subset of biology where competition occurs is in biofilms. Biofilms are a ubiquitous part of life. It has been estimated that 99.9% of bacteria grow in biofilms [3]. Biofilms are not harmless either; they can cause infections in medical implants which can lead to the death. They also can cause corrosion in oil in gas pipelines, which imposed an estimated cost of between \$3 billion to \$7 billion to oil and gas companies on maintenance and repair in 2001 [19]. A biofilm is created when enough of a certain species stick to some surface and start excreting an extracellular polymeric substance that binds the cells together, which is referred to as the biofilm matrix. Biofilms are a sessile collection of cells bound together by the extracellular polymeric substance that they produce. This structure that they create is bound to some surface or substratum

in a nutrient rich environment where the biofilm can continue to grow. Biofilms are typically not uniform in space or time and they can grow in aquatic and gas environments [2]. Since biofilms are so prevalent in nature, a deep body of research has been developed to study them. However, growing biofilms is often complicated and studying the interactions between the species can prove difficult. This is where a device called the chemostat comes in.

A chemostat is a laboratory device used to study the growth of bacteria and other microbes. It is also referred to as a continuous flow culture. In a chemostat, there are three tanks. The first tank holds some limiting substrates that are needed for microbial growth and are then pumped into the second tank. The second tank is where all of the reactions occur and the microbes grow. The final tank is a holding tank for all of the substrates and species that are swept out at some rate. This is needed so that tank two does not overflow. Biofilms are different from chemostats because the cells are bound together; they are not just floating in a tank. However, chemostats often provide a way to study how species interact without having to grow biofilms.

Bacteria that grow in biofilms and chemostats are often not just a single strain of species. Mutants evolve in bacteria all the time, and sometimes, they evolve into what is known as a cheater species. Cheaters are different from the original species in that they usually exploit some process carried out by the parent species. This type of social cheating has been demonstrated through experiments with Pseudomonas aeruginosa (PA) in [14]. When PA is grown in a lab with sodium caseinate as its carbon source, there are mutants that evolve that are quorum sensing deficient. Quorum sensing (QS) is a complicated process but can be thought of as a communication system between cells. The study found that wild-type PA are highly dependent on quorum sensing for growth, but the mutant cheaters who evolve from the wild-type are not as dependent on QS. The study found that this gives the mutant a competitive growth advantage over the wild-type [14]. Many studies have found that even when cheaters are present in a system, a tragedy of the commons can be avoided [1, 5, 6]. These examples establish that even when competition is present in a biological system, it does not always lead to the destruction of all the species involved.

The prevalence of competition in biology, and specifically biofilms and chemostats, has lead to the development of many mathematical models over the years. Mathematical modeling of competition between multiple species over a single limiting substrate goes back to 1977. In [8] a model was developed for a chemostat in which the most fit species wins and all the other species die off. Another particular mathematical model of a chemostat can be found in [15]. The model consists of two species, a substrate, enzyme, and nutrient. Species 1 is termed the cooperator and produces an enzyme that combines with the substrate to produce a nutrient that is needed by both species for survival. Species 2, termed the cheater does not produce this enzyme and just consumes produced nutrient. The model in [15] found that even with a low concentration of the cheater species present, both populations eventually die off from lack of nutrient. When the cheater was not present in the chemostat model, the cooperator persists and is able to keep reproducing [15]. This is similar to the basic model presented in [8], but represents a more complex interaction between substrates.

Since chemostats are often used to study what happens in biofilms, many mathematical models for multi-species biofilms have been developed. The first of which is credited to Wanner and Gujer in [20] called the biofilm accumulation model (BAM). This thesis seeks to adapt the chemostat model in [15] to a multi-species biofilm model using the techniques outlined in [20]. The idea is to compare this biofilm model that will be developed to the chemostat model in [15] and see if a tragedy of the commons still occurs. The model presented in this thesis will also be compared to other biofilm models that have been developed for competition between multiple species.

Our study begins in Chapter 2 which gives an overview of chemostats and how they are modeled. We then focus on the model in [15] and provide an overview of the work accomplished in this paper as well as replicate some numerical experiments. In Chapter 3, we discuss what biofilms are and give some examples of how competition in a biofilm has been previously modeled. Then we rigorously develop a new model for competition between two species in a biofilm and discuss

the numerical methods used to approximate solutions to the model. In Chapter 4, the results of the numerical simulations are presented. The results are then compared to another biofilm model in [10] as well as the model for the tragedy of the commons in the chemostat. In Chapter 5, we talk about various methods used to analyze the stability of the solutions obtained from the numerical experiments. Finally, we present a summary of the results and give our final thoughts on the differences between the biofilm model we have developed and the chemostat model in [15].

5

THE CHEMOSTAT

The Chemostat Model

Competition is especially pervasive in biology and understanding it is important to both mathematicians and biologists. Certain species like PA can cause lung infections and understanding how competition affects a population's survival could be crucial to remediating infections. There are two main types of competition in Biology: interference and exploitative. Interference competition is the direct interaction of two or more species competing for a resource in which they harm each other for the resource. Exploitative competition refers to at least two species competing for a common resource that is often needed for the survival of the individual species [16], but they do not fight each other.

An example of exploitative competition happens with PA. A strain of PA is grown that produces pyoverdine in a reduced iron environment where pyoverdine is important for growth. A second strain of PA is grown with the first and it lacks the means to produce pyoverdine, this species is the mutant cheater. The study [11] found that these species were able to co-exist in 56% of trials. This is an important result because mutant species evolve in biofilms all the time and understanding how the mutants interact with the biofilm can be important to understanding the survival of the species. Note that competition for public goods is not the only thing that can cause a biofilm to be compromised.

An example of interference competition can be seen in [21]. This study was done using Pseudomonas fluorescens (PF) with two different species in the biofilm. One species termed the cheater in this experiment creates a biofilm in the liquid broth phase of the biofilm and a cooperator species forms a biofilm at the broth air interface. The cheater species then invades the phase occupied by the cooperator. The study found that when these two species are grown together, the biofilms tended to be weaker and more prone to collapse [21].

As mentioned before, the chemostat is a device used to study the growth of different microbes

and can prove especially useful when studying competition. Chemostats consist of three tanks. The first tank contains substances that are needed for the microbes to grow. The substances in the first tank are pumped into the second tank at some rate referred to as the dilution rate. The second tank contains the species that are being studied and any products that they produce. This is the main tank and the growth and reactions that are being studied take place here. The species in tank two use the substances being pumped in from tank one as either a nutrient source or as a catalyst to produce a nutrient source. The third tank is a holding tank that contains all the products of tank two. Material is pumped out of tank two at the same dilution rate that substances are pumped in from tank one. This is necessary because as the substances are pumped in from tank one, there needs to be a drain so that tank two does not overflow. Thus the level of liquid in tank two remains constant. This continuous flow of material leads people to refer to a chemostat as a continuous flow culture. Chemostats provide a useful tool for studying competition between species because the amount of material needed for survival can be controlled, but they are also useful because they can easily be modeled mathematically.

The most basic chemostat model for competition that has been studied extensively consists of of a single limiting nutrient being pumped in from tank one and two species that live in the second tank [8]. Let N denote the nutrient. The species grow according to the Monod growth function $F_i(N) = \frac{\mu_i}{k_i+N}$. Each species uses the nutrient being pumped in for growth, but the Monod growth function associated to each species is different. Define $b_i := \frac{\mu_i}{D}$ to be the ratio of the maximum growth rate to the dilution rate, then the eventual outcome of this model is that the species with the lowest value of $\lambda_i = \frac{k_i}{b_i-1}$ will outcompete the other species [8]. Let X_1 and X_2 denote the two species. Then the model is described by the following equations

$$\frac{dN}{dt} = D(t)(N_0(t) - N) - \frac{1}{\gamma}(X_1 + X_2)F(N), \tag{2.1}$$

(2.2)

$$\frac{dX_1}{dt} = X_1(qF(N) - D(t)),, \tag{2.3}$$

$$\frac{dX_2}{dt} = X_2(F(N) - D(t)). \tag{2.4}$$

The function $D(t)$ is the dilution rate at which nutrient is pumped into the tank as well as the rate at which the species and nutrient are pumped out of the tank. $N_0(t)$ is the concentration of nutrient being pumped into the tank and the function $F(N) = \frac{\mu N}{k+N}$ is the Monod growth function which in this example is assumed to be the same for both species. The X_1 species is put at a disadvantage by the parameter q so that if $q < 1$, X_2 is more fit than X_1 and should win. The results can be seen in Figure 2.1. It can be seen that X_2 outcompetes X_1 and X_1 eventually dies off as expected due to the fact that X_2 has a growth advantage. This is to be expected due to the work in [8] on chemostat models for competition between multiple species and a single limiting nutrient.

The model presented in equations (2.1) - (2.4) has been adapted in [15]. In the chemostat model presented in [15], one limiting substrate is pumped in from tank one. Tank two holds two species. The first of which is termed the cooperator and produces an enzyme that combines with the substrate to produce a nutrient. The second species is termed the cheater and does not produce the enzyme, but still consumes the nutrient. The model in [15] provides another example for modeling competition in biology and specifically a chemostat.

The focus of the chemostat model presented in [15] is on exploitative competition. As previously mentioned, the model consists of two species, a substrate, an enzyme, and a nutrient. The cooperator will be denoted X_1. This is the species that produces an enzyme E that combines with a substrate S to produce a Nutrient N. The cooperator species is at a disadvantage because it must allocate some of its energy to producing this enzyme while also maintaining itself. The cheater species will be denoted by X_2 and does not produce the enzyme. The cheater species is at an advantage since it just consumes nutrient and does not need to allocate a portion of its growth to enzyme production. This is an example of exploitative competition. The competition is over which species can get the most nutrient needed for survival. This is a scenario in which a tragedy

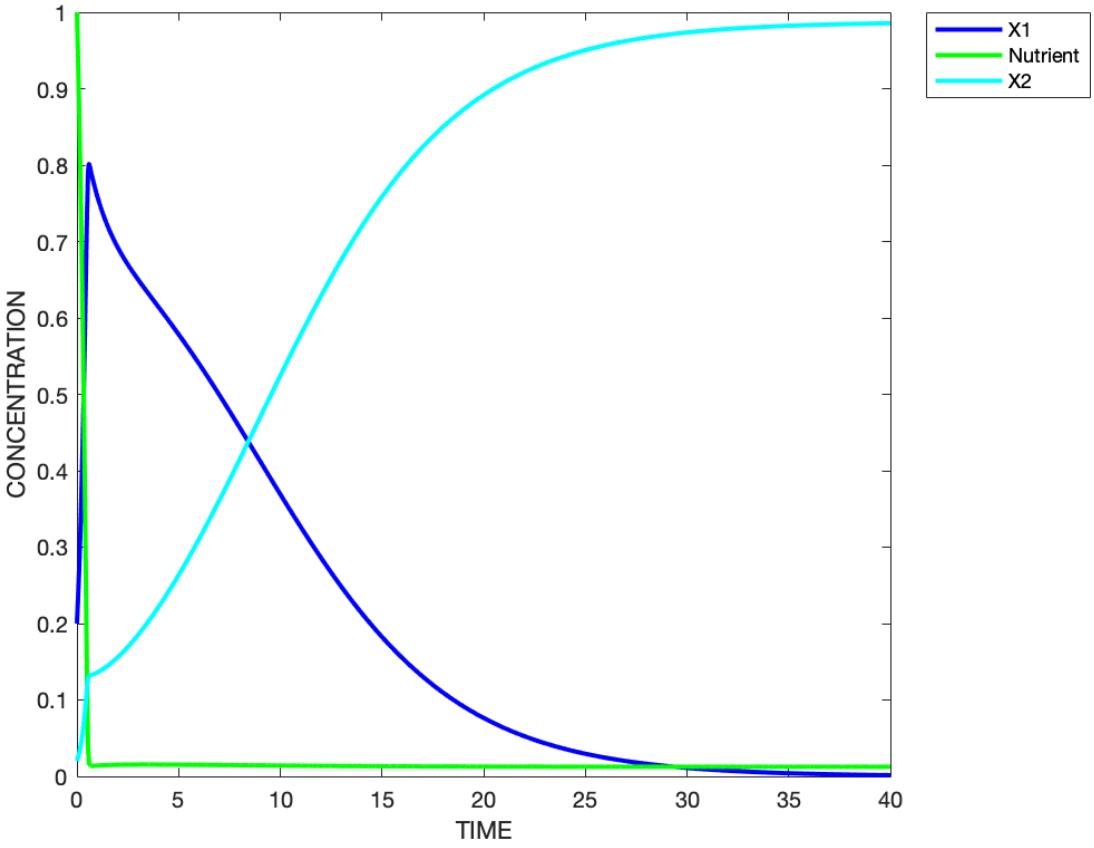

Figure 2.1: Numerical Simulation of equations (2.1) - (2.4) with $\mu = 5$, $k = .05$, $q = .8$, $D(t) = 1$, $N_0(t) = 1$, $\gamma = 1$ and initial conditions $N(0) = 1$, $X_1(0) = .2$ and $X_2(0) = .02$.

of the commons can occur.

To relate the model in [15] back to Hardin's example in his tragedy of the commons paper, the nutrient can be thought of as the grass that the cattle graze on. The two species represent the cattle owned by two different herdsmen. Here in this setup though, one of the species is making an effort to maintain the "commons" by producing an enzyme needed for nutrient production. This enzyme can be thought of as a fertilizer for the grass. The issue is that the cooperator species is doing all the work with no help; which ultimately leads to the tragedy. So the situation is slightly different but relates but relates back to Hardin's example, since the tragedy of the commons is ultimately

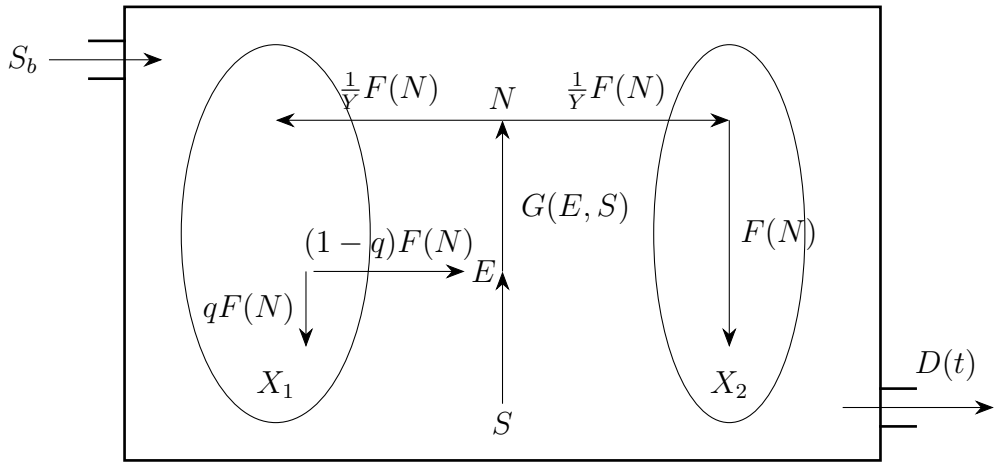

Figure 2.2: A schematic depicting the chemostat model for equations (2.5) - (2.9). The picture shows that S combines with E to produce N. N is then consumed by both X_1 and X_2 at a rate $\frac{1}{Y}F(N)$. X_1 produces E at a rate $(1-q)F(N)$. Finally X_1 grows at a rate $qF(N)$ and X_2 grows at a rate $F(N)$.

about exploitation of public goods.

The model is described by the following set of mass balance equations.

$$\frac{dS}{dt} = D(t)(S_0(t) - S) - G(E,S), \tag{2.5}$$

$$\frac{dN}{dt} = G(E,S) - \frac{1}{\gamma}(X_1 + X_2)F(N) - D(t)N, \tag{2.6}$$

$$\frac{dE}{dt} = (1-q)X_1F(N) - D(t)E, \tag{2.7}$$

$$\frac{dX_1}{dt} = X_1(qF(N) - D(t)), \tag{2.8}$$

$$\frac{dX_2}{dt} = X_2(F(N) - D(t)). \tag{2.9}$$

The values of X_1, X_2, S, E, and N represent dimensionless concentrations. Initial conditions for the components X_1, X_2, S, E, and N are specified in Figures 2.3 and 2.4

The function $G(E,S)$ is the rate at which the nutrient N is produced which depends on the concentration of the Enzyme E and substrate S . In [15], the function used for the production rate of the nutrient was $G(E,S) = aES$ where a is the rate constant that determines how E and S

combine. The Monod function $G(E,S) = S\frac{\mu_1 E}{k_1+E}$ where μ_1 is the maximum production rate and k_1 is the half saturation constant is also considered for the production of the nutrient as an extension to this study. The substrate is depleted at the rate $G(E,S)$. The function $F(N)$ which determines how nutrient is consumed and how each of the species grows is again a Monod growth function $F(N) = \frac{\mu N}{k_2+N}$. The rate at which the nutrient is consumed is $\frac{1}{\gamma}F(N)$ and is proportional to both of the species. The rate of consumption is the same for both of the species. The term $D(t)$ is the dilution rate at which the concentration of substrate S_0 is pumped in to the tank. The two species , substrate, enzyme, and the nutrient are also pumped out of the tank at a rate $D(t)$ proportional to their respective concentrations. The term $q \in (0,1)$ is a proportion of the growth term $F(N)$ that X_1 uses for its growth. This is the term that puts the cooperator at a disadvantage since the growth functions for X_1 and X_2 are the same. The other proportion $(1-q)$ is the proportion that X_1 uses to create the enzyme E. The term q is not an experimentally determined number for any specific species but rather a term that can be used to mathematically put the cooperator at a disadvantage.

This model leads to a tragedy where both of the species go extinct. The cooperator dies off first followed by a spike in the concentration of the cheater species who consumes all the nutrient and then eventually dies off since there is no more enzyme being produced by the cooperator to produce the nutrient. The results can be seen in Figures 2.3 and 2.4.

The behaviors exhibited by the species, nutrient, enzyme, and substrate are qualitatively the same for the two different $G(E,S)$ functions used. These results have been demonstrated numerically for $G(E,S) = aES$ in [15] and have now been replicated here. Figure 2.4 shows that a tragedy occurs when the Monod growth function $G(E,S) = S\frac{\mu_1 E}{k_1+E}$ is used for the nutrient production rate. This is to be expected as a consequence of the following assumptions and theorem.

Assumption 1: $G \in C^1$, $G(0,S) = G(E,0) = 0$ for all $E \geq 0$ and $S \geq 0$ and $F \in C^1$ with $F(0) = 0$

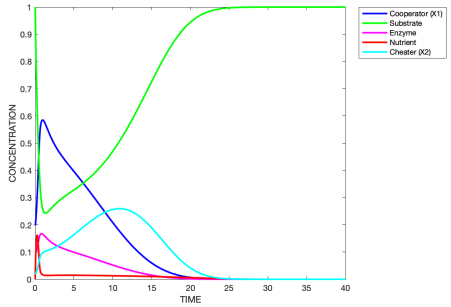

Figure 2.3: Time Simulation of equations equations (2.5) - (2.9) with $G = aES$, $F(N) = \frac{\mu_2 N}{k_2+N}$, $a = 20$, $k_2 = .05$, $\mu_2 = 5$, $D(t) = 1$, $q = .8$, $\gamma = 1$, $S_0 = 1$ with initial conditions $S(0) = 1$, $E(0) = .1$, $X_1(0) = .2$, $X_2(0) = .02$.

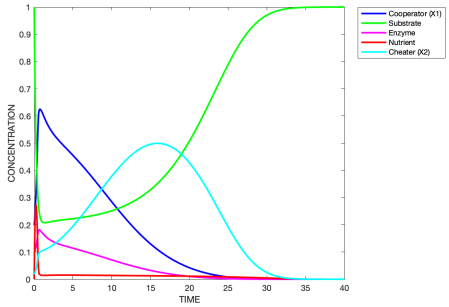

Figure 2.4: Time Simulation of equations equations (2.5) - (2.9) with $G = S\frac{\mu_1 E}{k_1+S}$, $F(N) = \frac{\mu_2 N}{k_2+N}$, $k_1 = .05$, $k_2 = .05$, $\mu_1 = 5$, $\mu_2 = 5$, $D(t) = 1$, $q = .8$, $\gamma = 1$, $S_0 = 1$ with initial conditions $S(0) = 1$, $E(0) = .1$, $X_1(0) = .2$, $X_2(0) = .02$.

Assumption 2: $D(t)$ and $S_0(t) \in C[0, \infty]$ and $S_0(t), D(t) > 0$ are bounded for all time.

Theorem 2.0.1. *Assume that assumptions 1 and 2 hold and assume that the initial conditions of (2.5) - (2.9) are such that $X_2(0) > 0$; that is the cheater is initially present. Then* $(N(t), E(t), X_1(t), X_2(t)) \to (0, 0, 0, 0)$ *as* $t \to \infty$

This theorem says that for suitably chosen growth functions $G(E, S)$ and $F(N)$ as well as suitable dilution $D(t)$ and bulk substrate $S_0(t)$ functions, that a tragedy of the commons will always occur with some initial cheater species present. This powerful result gives a whole class of models for which competition leads to extinction.

It is important to note that for this model, if there is no initial amount of the cheater species X_2 then, X_1 will persist and not die off. This is proven in [15]. A time simulation has also been run with $G(E, S) = S\frac{\mu_1 E}{k_1+E}$ and initial condition for the cheater species $X_2(0) = 0$ to provide a visual on what happens to the cooperator when there is no cheater present. The results are shown in Figure 2.5

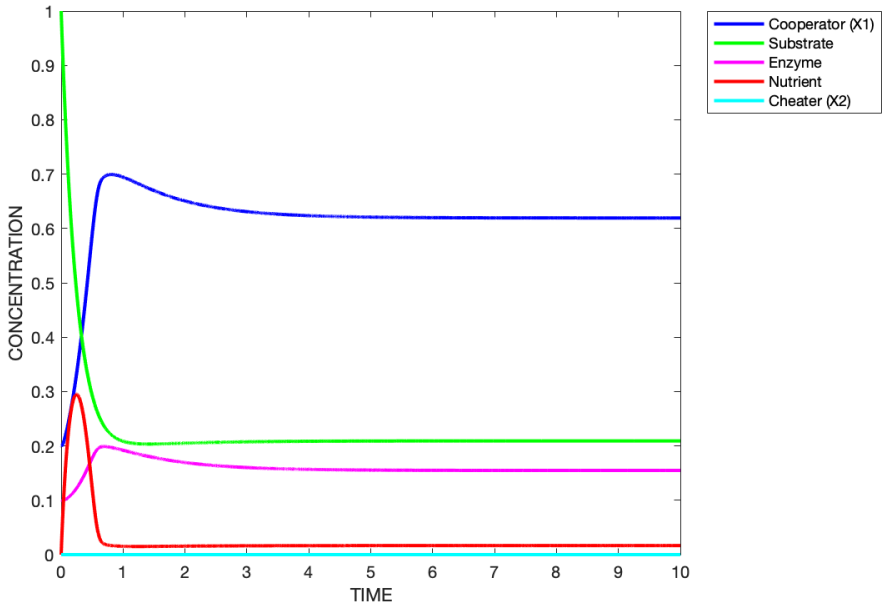

Figure 2.5: Time simulation with everything the same as in Figure 2.4 except $X_2(0) = 0$

The results shown in Figure 2.5 establish the important result that the extinction of X_1 is not determined by its dynamics, but rather its competition with the cheater species. The presence of the cheater species and the competition for resources is what ultimately causes the tragedy. Note that this is only a mathematical model and interactions among species are typically far more complicated than what is presented here. Under the conditions presented it has been shown that a tragedy of the commons is possible among competing species. This result is important for understanding interactions between microbial species where competition is often present. It may be useful to know what competition does to certain species such as PA which can cause lung infections in humans. Understanding conditions in which PA may not be able to survive could be critical in understanding how to fight these infections.

13

THE BIOFILM MODEL

Biofilms and Models

Biofilm models have been around since the 1980's and have continued to develop over the years. They have been modeled mathematically since 1986 when Wanner and Gujer developed the first multispecies biofilm model known as the biofilm accumulation model (BAM) [20]. A biofilm differs from a chemostat because it is anchored to some surface. The microbes are not just floating around in a tank like the chemostat. This leads to the definition of a biofilm as a community of cells immobilized at a substratum. The cells are bound together in an extracellular polymeric substance that they produce known as the biofilm matrix. Biofilms accumulate on different surfaces and are not necessarily uniform in time or space [2]. Biofilms typically grow in aquatic environments, where they can use the nutrients in their surrounding environment to grow. Sometimes the microorganisms in biofilms produce their own enzymes that combine with other molecules in the surrounding environment to produce a nutrient needed for growth. Note that sometimes biofilms can grow in a gas environment. Altogether, a biofilm system consists of the biofilm, an overlying liquid or gas layer, and a substratum that the biofilm is attached to [2]. In this thesis, the focus will be on biofilms grown in liquid environments. So the overlaying liquid layer will be referred to as the bulk liquid biofilm interface (see Figure 3.1).

Biofilms typically grow in high shear environments. A high shear environment is one where the flow of a liquid is swift. This may seem contradictory as one would tend to think that a faster moving medium would sweep away a biofilm, but it is observed that many biofilms can grow in environments with Reynolds's numbers as high as 5000 [3]. The Reynolds's number is an indicator on how fast a fluid is flowing. Higher Reynolds's numbers mean that the flow is more likely to be turbulent and lower numbers suggest a more laminar flow. The flow over a biofilm can be modeled using different types of boundary conditions which will be explored in this Chapter. Robin conditions will be used to simulate water flowing over the biofilm at different speeds and

Dirichlet boundary conditions will be used to simulate stagnant water at the biofilm bulk liquid interface. Biofilms are typically heterogeneous structures in which layers of different species tend to form [3]. This is another difference from a chemostat. In a biofim, a species may form at a high concentration near the bottom while a different species may be more prevalent at a different height in the biofilm. This is one of the reasons to explore the model in [15], by adding a spatial dimension and seeing if the tragedy of the commons still occurs.

Before the derivation of the model is presented, some important work that has been done in modeling biofilm competition by Klapper and Szmolay in [10] is discussed. In [10] two species compete for a substrate, one species performs better in low substrate concentrations, while the other performs better in high substrate concentrations. This is determined by a set of reaction advection equations for the species. The growth terms for each species are Monod and are chosen so that the growth rate of species 1 will be faster at high concentrations of substrate and species 2 will grow faster at lower concentrations of substrate. For example, if the Monod growth function for the species is

$$g_j(C_1) = r_j \frac{C_1}{k_j + C_1}.$$

Then $r_1 = 1$, $k_1 = 1$ and $r_2 = .5$, $k_2 = .15$ [10]. Where C_1 represents the concentration of the substrate. So, it can be seen that species 1 will have a larger growth rate than species 2 at high concentrations of C_1 and species 2 will have a larger growth rate at lower concentrations of C_1. This differs from the model that will be presented in this thesis since it will be assumed that the growth functions for the cooperator and cheater are the same, and the cooperator will be put at a disadvantage by the factor q. This paper finds that when advection is the only transport process for the species, the species will die off unless they can survive at the base of the biofilm. It is also found that if a small amount of downward diffusion is added to the reaction-advection equations for the species, then both species can persist. This model establishes the important result that for cooperation in biofilms, some amount of mobility within the biofilm is necessary.

Another example that bears some resemblance to the model that will be developed in this thesis can be seen in [4]. This study develops a mathematical model for Pseudomonas fluorescens (PF) in an iron-scarce environment. Iron is is often necessary for the growth of certain microbes, but there are many circumstances in which iron is scarce. When iron is scarce, PF produces a siderophore that can be used to trap iron for later consumption. The species of PF that can produce siderophore is termed the chelator. This siderophore essentially provides a way for PF to scavenge the iron in a given environment. However, there are some species of PF that cannot scavenge the iron entrapped in the siderophore. In this study, this species is referred to as the non-chelator. The non-chelator cannot use the iron trapped by the siderophore. This is what sets up the competition in the biofilm. The chelator can use iron in the environment and also use the iron that has been trapped by the siderophore. The non-chelator can only use iron that is not trapped by the siderophore. This difference gives the chelator an advantage in the biofilm since it can set aside iron for its own use. This is a crucial difference between the model presented in [15], where the nutrient produced by the enzyme can be used by both species. The study found that the chelator outcompetes the non-chelator and is able to maintain a higher volume fraction because of its iron-scavenging advantage. The eventual outcome of the numerical simulations is that the non-chelator dies out [4].

To get an idea of how a biofilm is typically modeled, see Figure 3.1. In this figure, the red and green ovals represent some species in the biofilm and the grey ovals represent some nutrient that they are using for growth. The hexagonal pattern represents that these species are bound together to form the biofilm matrix. The blank white space represents a liquid that the biofilm grows in. The biofilm liquid interface is represented by where the hexagonal pattern meets the white blank space. The biofilm matrix is growing in the z direction and propagates further into the bulk liquid which creates a moving boundary. Note that this picture represents growth in one spatial dimension.

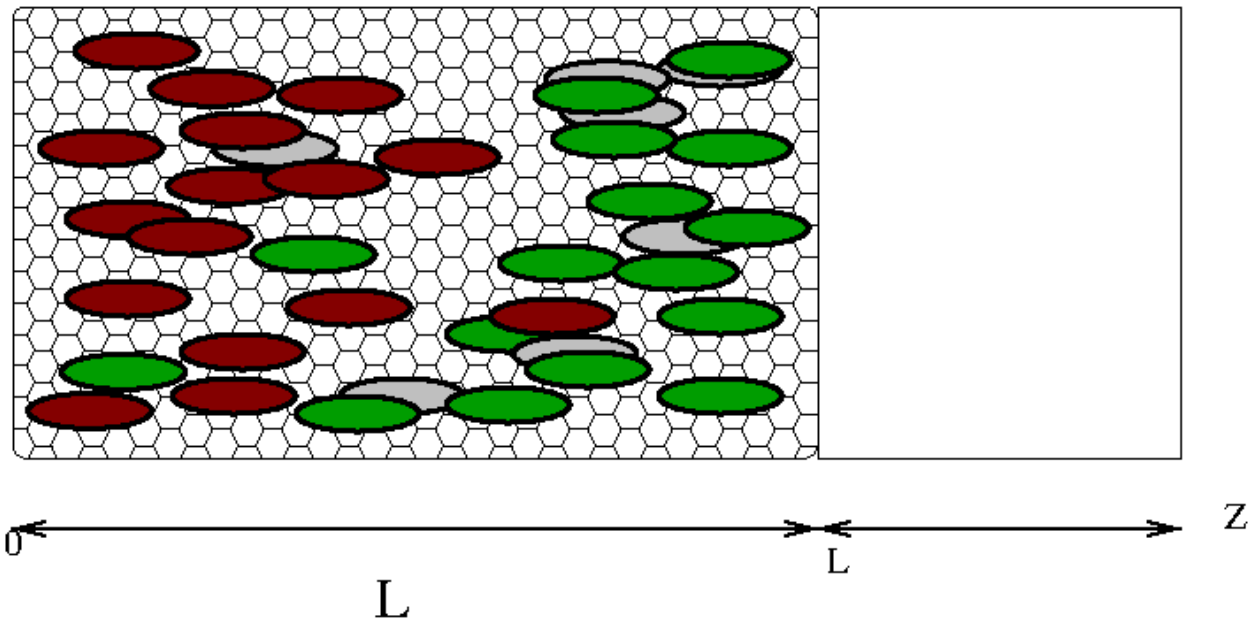

Figure 3.1: Typical Depiction of how a one dimensional biofilm is modeled.

The Model

The model will be based off of the biofilm accumulation model developed by Wanner and Gujer in 1986 [20]. The biofilm model will consist of the cooperator and cheater species, as well as an enzyme, nutrient, and substrate. The cooperator will produce the enzyme necessary to make the nutrient when it combines with the substrate. Both the cooperator and the cheater will consume the nutrient. Therefore, the model reflects the same interactions that occur in the chemostat model in [15]. It is assumed that a 1-dimensional spatial model is sufficient for the situation. The spatial coordinate will be z and the time coordinate t. There are some assumptions that will have to be used so that this situation can be modeled mathematically. They are listed in Table 3.1.

It is assumed that the biofilm is made up of a single solid phase occupied by the cooperator and cheater and one liquid phase. For this model, the nutrient, enzyme, and substrate will be assumed to to in the liquid phase and will be referred to as the dissolved components. To model the structure of the biofilm, volume fractions are used. A volume fraction is just a proportion of the

Table 3.1: Assumptions in BAM

Assumption	Description
A1	The biofilm is a continuum model. This is so that components can be described by concentrations instead of individual particles.
A2	The biofilm can be assumed to grow in only one direction.
A3	The biofilm consists of a liquid phase and a solid phase.
A4	The solid phases are bound so that they form a continuous structure
A5	The volume fraction ϵ_ℓ is constant
A6	Advective transport of the solid phases is the result of volume changes in the solid phases.
A7	The Advective velocities for all the solid phases are assumed to be the same.
A8	The liquid phase contains only dissolved components.
A9	Transport of the dissolved components in the liquid phase is by molecular diffusion; Fick's First law of diffusion describes Molecular diffusion.
A10	The solid phase contains no dissolved or suspended components.
A11	The advective velocities for both species are the same.

biofilm that is occupied by a solid or liquid phase. Following the same notation as in Chapter 2, the cooperator will be denoted X_1 and the cheater by X_2. The species are quantified using volume fractions which are dimensionless. The first condition that needs to be imposed is that the volume fraction of both the species sum to $1 - \epsilon_\ell$,

$$X_1 + X_2 = 1 - \epsilon_\ell. \tag{3.1}$$

The term ϵ_ℓ is the constant fraction of the biofilm that is occupied by the liquid and is assumed to be small for this model. This says that the volume taken up by the dissolved components (enzyme, substrate, and nutrient) is small when compared to the volume taken up by the solid phase. In other words, the biofilm matrix is mostly made up of the solid phase. The substrate will be denoted by S, the enzyme by E and the nutrient by N. The substrate, nutrient and enzyme occupy the liquid volume fraction and diffuse through the biofilm. Instead of modeling the dissolved components as volume fractions, they can be thought of as concentrations in the liquid phase. For this model, it is assumed that the concentrations are dimensionless and are intended to give a qualitative behavior for what the dissolved components will do within the biofilm.

The mass balance equation is used to describe the evolution of the volume fractions of the species. Let ρ be the density of each species. The density is assumed to be constant and equal for both species. The concentration of the species is then given by ρX_i for $i = 1, 2$. It is assumed that the biofilm grows due to volume changes and that the main transport process for the solid phase is due to advection. So, the species that make up the solid phase move through the biofilm at some velocity v. Flux due to advection is given by

$$J = vX_i\rho \quad \text{for i = 1,2.}$$

It is assumed that the velocity for the two species in the solid phase are the same. Thus the mass

balance equations for the two species are given by

$$\frac{\partial(\rho X_1)}{\partial t} = -\frac{\partial(\rho X_1 v)}{\partial z} + q\rho X_1 F(N), \tag{3.2}$$

$$\frac{\partial(\rho X_2)}{\partial t} = -\frac{\partial(\rho X_2 v)}{\partial z} + \rho X_2 F(N), \tag{3.3}$$

where $F(N)$ is some production function that accounts for the growth of both of the species and depends of the amount of nutrient in the biofilm. The parameter $q \in (0, 1)$ is a fraction that tells us how much energy X_1 allocates for its own growth. This parameter q is the same parameter that was used in [15] to impose a burden on the growth of X_1. Since it has been assumed that the species have the same constant density ρ, equations (3.2) and (3.3) can be simplified by dividing through by ρ.

Now that the governing equations for the species have been established, an equation for the velocity is needed. To obtain an equation for the velocity, sum equations (3.2) and (3.3) to get

$$\frac{\partial(X_1 + X_2)}{\partial t} + \frac{\partial}{\partial z}\left(v(X_1 + X_2)\right) + = F(N)(qX_1 + X_2). \tag{3.4}$$

Equation (3.1) says that the sum of the volume fractions of both species is constant , so equation (3.4) simplifies to

$$\frac{\partial v}{\partial z} = \frac{F(N)(qX_1 + X_2)}{1 - \epsilon_\ell}. \tag{3.5}$$

The equation for the velocity says that the divergence of the velocity is equal to the sum of the growth rates for the two species divided by the volume fraction occupied by the solid phase. Equation (3.5) can be integrated with respect to z to obtain the velocity

$$v = \int_0^z \frac{F(N)(qX_1 + X_2)}{1 - \epsilon_\ell} ds. \tag{3.6}$$

To solve this system of equations, there needs to be a boundary condition for the interface between the solid phase of the biofilm and the bulk liquid (see Figure 3.1). This boundary condition can be obtained by relating the time rate change of the biofilm thickness $L(t)$ to the velocity of the biofilm at the interface which will be denoted by v_I. It is assumed that there is detachment in the model so that some of the biofilm is eroded away over time. Detachment is the process that balances the growth of biofilms and helps determine steady state accumulation of the biofilm [17]. The main processes in detachment are erosion, sloughing, human intervention, predator grazing and abrasion [17]. When including detachment the equation for the progression of the biofilm thickness will be as follows

$$\frac{dL}{dt} = v_I - \sigma L^2(t), \tag{3.7}$$

$$L(0) = L_I. \tag{3.8}$$

The initial condition $L(0) = L_I$ says that the biofilm starts at some constant thickness. The σL^2 is the detachment term and implies that the biofilm thickness is finite, which is what one would expect in the real world. The detachment term used used here σL^2, is the one used for microbial growth [17]. Note that equation (3.7) implies a moving boundary.

To deal with the moving boundary, the following change of variables is made. This change of variables will let $\tilde{z} \in [0, 1]$ and thus gives a fixed spatial boundary. So let

$$z = \tilde{z}L(t).$$

Now for an arbitrary function $f(z, t)$, the chain rule yields the following,

$$\frac{\partial f}{\partial z} = \frac{\partial f}{\partial \tilde{z}} \frac{1}{L(t)},$$

and

$$\begin{aligned}\frac{\partial f(z,t)}{\partial t} &= \frac{\partial f(\tilde{z},t)}{\partial t} + \frac{\partial f(\tilde{z},t)}{\partial \tilde{z}}\frac{\partial \tilde{z}}{\partial t},\\ &= \frac{\partial f(\tilde{z},t)}{\partial t} + \frac{\partial f(\tilde{z},t)}{\partial \tilde{z}}\frac{-z}{L^2(t)}\frac{dL}{dt},\\ &= \frac{\partial f(\tilde{z},t)}{\partial t} - \frac{\partial f(\tilde{z},t)}{\partial \tilde{z}}\frac{\tilde{z}}{L(t)}\frac{dL}{dt}.\end{aligned}$$

The next thing that needs to be considered is the governing equations and boundary conditions for the substrate S, the produced nutrient N, and the enzyme E. The main transport process for the enzyme, nutrient, and substrate is diffusion. The governing equations will be the following without the spatial change of variables,

$$\frac{\partial S}{\partial t} = D\frac{\partial^2 S}{\partial z^2} - G(E,S), \tag{3.9}$$

$$\frac{\partial E}{\partial t} = D\frac{\partial^2 E}{\partial z^2} + (1-q)F(N)X_1, \tag{3.10}$$

$$\frac{\partial N}{\partial t} = D\frac{\partial^2 N}{\partial z^2} + G(E,S) - \frac{1}{\gamma}\rho(X_1+X_2)F(N). \tag{3.11}$$

After taking into account the change of variables for the spatial dimension, the equations will be

$$\frac{\partial S}{\partial t} - \frac{\partial S}{\partial z}\frac{dL}{dt}\frac{z}{L(t)} = \frac{D}{L^2(t)}\frac{\partial^2 S}{\partial x^2} - G(E,S), \tag{3.12}$$

$$\frac{\partial E}{\partial t} - \frac{\partial E}{\partial z}\frac{dL}{dt}\frac{z}{L(t)} = \frac{D}{L^2(t)}\frac{\partial^2 E}{\partial x^2} + (1-q)F(N)X_1, \tag{3.13}$$

$$\frac{\partial N}{\partial t} - \frac{\partial N}{\partial z}\frac{dL}{dt}\frac{z}{L(t)} = \frac{D}{L^2(t)}\frac{\partial^2 N}{\partial x^2} + G(E,S) - \frac{1}{\gamma}(X_1+X_2)F(N). \tag{3.14}$$

The set of equations (3.12) - (3.14) are reaction diffusion equations that describe how the dissolved components act in the biofilm. The substrate combines with the enzyme produced by X_1 to make the produced nutrient N. This reaction is described by a function that will be denoted $G(E,S)$. In the chemostat model [15], the function $G(E,S) = aES$ was used, but a Monod

function $G(E,S) = S\frac{\mu_1 E}{k_1+E}$ is considered for this model. The substrate diffuses through the biofilm and is converted to nutrient at some rate proportional to the growth of the the enzyme.

Next consider the governing equation (3.13) for the enzyme. The enzyme behaves in a similar way to the substrate. It diffuses throughout the biofilm and is produced at a rate $F(N)$ proportional to X_1. The factor $(1-q)$ determines how much enzyme is produced and is used to qualitatively represent the burden that X_1 must bear in producing the enzyme necessary for survival. Notice that $(1-q)$ is the other part of the proportion q that determined the growth of X_1. So here this proportion $(1-q)$ is a qualitative representation of how much energy X_1 must expend to produce the enzyme.

Finally consider equation (3.14) for the produced nutrient. This is similar to the equations for the substrate and enzyme. The nutrient is consumed at a rate $F(N)$ proportional the the volume fractions of the cheater and cooperator species. The yield of the process is denoted by γ, so the consumption rate of the produced nutrient is $\frac{1}{\gamma}F(N)$. The reaction term for production of the nutrient is the same reaction term that corresponds to the conversion of substrate into nutrient. The only difference is that $G(E,S)$ is positive in this equation. This says that the the nutrient is produced at a rate $G(E,S)$. The diffusion coefficients D, for the dissolved components are all assumed to be the same, since these molecules are assumed to all have similar properties and are diffusing through the same medium.

The boundary conditions for the dissolved components in the biofilm will be of the Neumann type at the left boundary, $z = 0$. This says that there is no flux at this boundary. This boundary can be thought of as the bottom of a petri dish where it would be impossible for any of the dissolved components to leak out of. Two separate cases are considered for the right boundary at $z = 1$. The first case is that the boundary between the biofilm and bulk fluid corresponds to Dirichlet boundary conditions. At the boundary $z = 1$ each dissolved component will have a constant concentration at the bulk fluid biofilm interface (see Figure 3.1). It is assumed that the concentration of E and N at the bulk liquid biofilm interface are constant concentrations of 0. This says that there is no

extraneous nutrient or enzyme floating out in the bulk liquid. The Substrate is assumed to have some constant concentration at the boundary $Sb > 0$. Essentially this says that there must be some place where the substrate comes from. Mathematically, this creates a positive gradient into the biofilm which corresponds to a replenishment of substrate throughout the biofilm matrix. The boundary conditions will then be

$$\frac{\partial S}{\partial z}\Big|_{z=0} = 0 \qquad S(1,t) = Sb, \tag{3.15}$$

$$\frac{\partial E}{\partial z}\Big|_{z=0} = 0 \qquad E(1,t) = 0, \tag{3.16}$$

$$\frac{\partial N}{\partial z}\Big|_{z=0} = 0 \qquad N(1,t) = 0. \tag{3.17}$$

The Dirichlet boundary conditions correspond to some large amount of substrate in the bulk fluid. If this is not included then the enzyme will quickly combine with the substrate that is initially in the biofilm to produce some nutrient. This small amount of nutrient produced would be rapidly consumed by the two species and little growth would occur. Thus, this bulk concentration of substrate in the bulk liquid phase is needed so that the biofilm can sustain itself. Essentially the substrate is the limiting factor needed from the outside environment and the bulk liquid does not have any enzyme so that the production of enzyme is exclusively on the cooperator.

Another type of boundary condition that is used to model biofilm growth is the Robin boundary condition. This condition corresponds to a layer of liquid moving over the biofilm at different speeds. This boundary condition is hypothetical in the sense that is does not model real world empirical results, but can be used to simulate flowing liquid over a biofilm [4]. The Robin

boundary conditions at the biofilm bulk liquid interface $z = 1$ are as follows

$$D\frac{\partial S}{\partial z}\Big|_{z=0} = 0 \qquad \frac{D}{L(t)}\frac{\partial S}{\partial z}\Big|_{z=1} = \beta(Sb - S), \tag{3.18}$$

$$D\frac{\partial E}{\partial z}\Big|_{z=0} = 0 \qquad \frac{D}{L(t)}\frac{\partial E}{\partial z}\Big|_{z=1} = -\beta E, \tag{3.19}$$

$$D\frac{\partial N}{\partial z}\Big|_{z=0} = 0 \qquad \frac{D}{L(t)}\frac{\partial N}{\partial z}\Big|_{z=1} = -\beta N. \tag{3.20}$$

The parameter β is a number that is related to the velocity of the flow over the biofilm. It is a positive constant. Smaller values of β correspond to a slower flow rate over the biofilm interface and larger values of β indicate a faster flow rate over the bulk liquid biofilm interface. Again, Sb is the concentration of substrate in the bulk water, but now for sufficiently large values of Sb, the gradient of the substrate at $z = 1$ will be positive and substrate will flow into the biofilm. The flux for the nutrient and enzyme is negative because there is no enzyme or nutrient in the bulk liquid, so the enzyme and nutrient leak out into the bulk liquid. Note that the Dirichlet boundary conditions can be recovered from equations (3.18) - (3.20) if $\beta \to \infty$.

The full system of equations can now be presented. The change of variables $z = \tilde{z}L(t)$ has already been applied for the dissolved components and after applying it to equations (3.2), (3.3), and (3.5), the system will be

$$\frac{\partial X_1}{\partial t} - \frac{\partial X_1}{\partial z}\frac{dL}{dt}\frac{z}{L(t)} + \frac{1}{L(t)}\frac{\partial}{\partial z}(vX_1) = qF(N)X_1, \tag{3.21}$$

$$\frac{\partial X_2}{\partial t} - \frac{\partial X_2}{\partial z}\frac{dL}{dt}\frac{z}{L(t)} + \frac{1}{L(t)}\frac{\partial}{\partial z}(vX_2) = F(N)X_2, \tag{3.22}$$

$$\frac{\partial S}{\partial t} - \frac{\partial S}{\partial z}\frac{dL}{dt}\frac{z}{L(t)} = \frac{D}{L(t)^2}\frac{\partial^2 S}{\partial x^2} - G(E,S), \tag{3.23}$$

$$\frac{\partial E}{\partial t} - \frac{\partial E}{\partial z}\frac{dL}{dt}\frac{z}{L(t)} = \frac{D}{L(t)^2}\frac{\partial^2 E}{\partial x^2} + (1-q)F(N)X_1, \tag{3.24}$$

$$\tag{3.25}$$

$$\frac{\partial N}{\partial t} - \frac{\partial N}{\partial z}\frac{dL}{dt}\frac{z}{L(t)} = \frac{D}{L(t)^2}\frac{\partial^2 N}{\partial x^2} + G(E,S) - \frac{1}{\gamma}(X_1 + X_2)F(N), \tag{3.26}$$

$$\frac{\partial v}{\partial z}\frac{1}{L(t)} = \frac{F(N)(qX_1 + X_2)}{(1-\epsilon_\ell).} \tag{3.27}$$

Another simplification that will be made in the model is to assume that the dissolved components will equilibrate to a steady state rapidly, so it is assumed that all three are in a quasi-steady state. This will make the system easier to solve because the system of equations is considered stiff. This means that certain variables respond orders of magnitude faster than other variables in the system. The argument for why this dissolved components can be assumed to be in a quasi-steady state is presented below. First some parameters are introduced to begin the simplification. Let $L_A = 3 \times 10^{-3} cm$ be the average thickness of the biofilm. This is a typical value for PA grown in a lab [18]. It is important to note that $L_A \neq L(t)$. The Growth function for the two species in now assumed to be of the Monod type so that $F(N) = \frac{\mu_2 N}{k_2 + N}$. Let $\mu_2 = 10^0 \text{day}^{-1}$ be the maximum specific growth rate. Now define the dimensionless variables,

$$t = \frac{\hat{t}}{\mu_2} \qquad v = \hat{v}\mu_2 L_A \qquad z = \hat{z} L_A.$$

Then substitute these variables into equation (3.2) and arrive at the following

$$\mu_2 \frac{\partial X_1}{\partial \hat{t}} = -\frac{1}{L_A}\frac{\partial (X_1 \hat{v} \mu L_A)}{\partial \hat{z}} + qX_1 F(N).$$

Now divide through by μ_2 and arrive at the dimensionless equation,

$$\frac{\partial X_1}{\partial \hat{t}} = -\frac{\partial (X_1 \hat{v})}{\partial \hat{z}} + qX_1 \frac{N}{k+N}.$$

The same change of variables is then applied to equation (3.26) for the produced nutrient

N. To keep things simple, it will be demonstrated that the time it takes for the nutrient to change is small and realized that the same change of variables could be applied to the equation for the enzyme and substrate to yield the same results. Also, let $N = N_0\hat{N}$, where N_0 is the concentration of the nutrient at the interface between the biofilm and the liquid phase. So applying the change of variables to equation (3.26), will yield the following

$$\mu_2 N_0 \frac{\partial \hat{N}}{\partial \hat{t}} = \left(\frac{N_0 D}{L_A^2}\right)\frac{\partial^2 N}{\partial \hat{z}^2} + G(E,S) - \frac{1}{\gamma}(X_1 + X_2)\left(\mu_2 \frac{NN_0}{k + NN_0}\right).$$

Now factor out an N_0 from the denominator of $\mu_2 \frac{NN_0}{k+NN_0}$ and divide the equation through by $\frac{N_0 D}{L_A^2}$ which will yield

$$\left(\frac{\mu_2 L_A^2}{D}\right)\frac{\partial \hat{N}}{\partial \hat{t}} = \frac{\partial^2 N}{\partial \hat{z}^2} + \left(\frac{L_A^2}{DN_0}\right)G - \frac{1}{\gamma}(X_1 + X_2)\left(\frac{\mu_2 L_A^2}{DN_0}\right)\frac{N}{\frac{k}{N_0} + N}.$$

Then consider the magnitude of $\frac{\mu_2 L_A^2}{D}$. An average diffusion coefficient for PA has units $[D] = \frac{1\times 10^{-8}\text{cm}^2}{\text{second}}$. First convert μ_2 so that the rate is in seconds and get $\mu_2 = 8.64 \times 10^{-4}\text{seconds}^{-1}$ So, if the calculation of $\frac{\mu_2 L_A^2}{D}$ is carried out with average values, then $\frac{\mu_2 L_A^2}{D}$ is on the order of

$$\frac{\mu_2 L_A^2}{D} = .01.$$

The above argument indicates that the dissolved components can be modeled using a quasi-steady state approximation. The full model can now be developed to compare the differences in a biofilm to the chemostat in [15].

So, the system of equations will be the following if it is assumed that the dissolved

components are in steady state and the change of variables for the spatial dimension is applied

$$\frac{\partial X_1}{\partial t} - \frac{\partial X_1}{\partial z}\frac{dL}{dt}\frac{z}{L(t)} + \frac{\partial v}{\partial z}\frac{X_1}{L(t)} + v\frac{\partial X_1}{\partial z}\frac{1}{L(t)} = \frac{q\mu_2 N}{k_2+N}X_1, \tag{3.28}$$

$$\frac{\partial X_2}{\partial t} - \frac{\partial X_2}{\partial z}\frac{dL}{dt}\frac{z}{L(t)} + \frac{\partial v}{\partial z}\frac{X_2}{L(t)} + v\frac{\partial X_2}{\partial z}\frac{1}{L(t)} = \frac{\mu_2 N}{k_2+N}X_2, \tag{3.29}$$

$$\frac{D}{L(t)^2}\frac{\partial^2 S}{\partial x^2} - S\frac{\mu_1 E}{k_1+E} = 0, \tag{3.30}$$

$$\frac{D}{L(t)^2}\frac{\partial^2 E}{\partial x^2} + \frac{(1-q)\mu_2 N}{k_2+N}X_1 = 0, \tag{3.31}$$

$$\frac{D}{L(t)^2}\frac{\partial^2 N}{\partial x^2} + S\frac{\mu_1 E}{k_1+E} - \frac{1}{\gamma}(X_1+X_2)\frac{\mu_2 N}{k_2+N} = 0, \tag{3.32}$$

$$\frac{\partial v}{\partial z}\frac{1}{L(t)} = \frac{\mu_2 N}{(k_2+N)(1-\epsilon_\ell)}(qX_1+X_2). \tag{3.33}$$

The following initial conditions are used for the system of equations. It is assumed that there is initially a small amount of enzyme concentration in the system like the chemostat model in [15]. Also the initial volume fraction of X_2 is forced to be $1 - X_I - \epsilon_\ell$ for some initial volume fraction of the cooperator X_I.

$$S(z,0) = 0 \tag{3.34}$$

$$N(z,0) = 0 \tag{3.35}$$

$$E(z,0) = E_I \tag{3.36}$$

$$X_1(z,0) = X_I \tag{3.37}$$

$$X_2(z,0) = 1 - X_I - \epsilon_\ell \tag{3.38}$$

The system of equations (3.28) - (3.33) is the basic model. To make the model a bit more realistic, death terms for the two species can be added. To do this, consider a third reaction advection equation that keeps track of the dead cells. The dead cells will be denoted by X_3. Now equation (3.1) will become

$$X_1 + X_2 + X_3 = 1 - \epsilon_\ell. \tag{3.39}$$

The death terms for X_1 and X_2 will correspond to a linear term that is subtracted from the reaction terms in equations (3.28) and (3.29) so that they now read

$$\frac{\partial X_1}{\partial t} - \frac{\partial X_1}{\partial z}\frac{z}{L(t)}\frac{dL}{dt} + \frac{1}{L(t)}\frac{\partial}{\partial z}\left(vX_1\right) = \frac{qmN}{a+N}X_1 - d_1X_1, \tag{3.40}$$

$$\frac{\partial X_2}{\partial t} - \frac{\partial X_2}{\partial z}\frac{z}{L(t)}\frac{dL}{dt} + \frac{1}{L(t)}\frac{\partial}{\partial z}\left(vX_2\right) = \frac{mN}{a+N}X_2 - d_2X_2. \tag{3.41}$$

This model corresponds to a loss of cooperator and cheater species proportional to the death constants d_1 and d_2 respectively. The reaction advection equation that keeps track of the dead cells will then be,

$$\frac{\partial X_3}{\partial t} - \frac{\partial X_3}{\partial z}\frac{z}{L(t)}\frac{dL}{dt} + \frac{1}{L(t)}\frac{\partial}{\partial z}\left(vX_3\right) = d_1X_1 + d_2X_2. \tag{3.42}$$

As one can see the equation for the dead cells is just another reaction advection equation where the reaction terms are just the sum of the dead cooperator and cheater species. This equation does not change the velocity because if equations (3.40), (3.41) and (3.42) are summed, the newly introduced death terms will all cancel each other out and the velocity will still be dependent on the growth terms for the cooperator and cheater. The death terms can be thought of as similar to the dilution rate for the chemostat model. In the chemostat, the cooperator and cheater flow out of the chemostat proportional to some constant dilution rate and now a similar term that is called death is included in equations (3.40) and (3.41). The only difference is that instead of the species being swept out of the chemostat, the dead cells are kept track of by using equation (3.42).

Numerical Methods

The solutions to the model will have to be approximated using numerical methods. The code used can be found as a downloadable file on ScholarWorks. To recap, the model that has been derived without death terms is as follows and various numerical methods will be implemented to come up with approximate solutions

$$\frac{\partial X_1}{\partial t} - \frac{\partial X_1}{\partial z}\frac{dL}{dt}\frac{z}{L(t)} + \frac{\partial v}{\partial z}\frac{X_1}{L(t)} + v\frac{\partial X_1}{\partial z}\frac{1}{L(t)} = \frac{q\mu_2 N}{k_2+N}X_1, \tag{3.43}$$

$$\frac{\partial X_2}{\partial t} - \frac{\partial X_2}{\partial z}\frac{dL}{dt}\frac{z}{L(t)} + \frac{\partial v}{\partial z}\frac{X_2}{L(t)} + v\frac{\partial X_2}{\partial z}\frac{1}{L(t)} = \frac{\mu_2 N}{k_2+N}X_2, \tag{3.44}$$

$$\frac{D}{L(t)^2}\frac{\partial^2 S}{\partial x^2} - S\frac{\mu_1 E}{k_1+E} = 0, \tag{3.45}$$

$$\frac{D}{L(t)^2}\frac{\partial^2 E}{\partial x^2} + \frac{(1-q)\mu_2 N}{k_2+N}X_1 = 0, \tag{3.46}$$

$$\frac{D}{L(t)^2}\frac{\partial^2 N}{\partial x^2} + S\frac{\mu_1 E}{k_1+E} - \frac{1}{\gamma}(X_1+X_2)\frac{\mu_2 N}{k_2+N} = 0, \tag{3.47}$$

$$\frac{\partial v}{\partial z}\frac{1}{L(t)} = \frac{\mu_2 N}{(k_2+N)(1-\epsilon_\ell)}(qX_1+X_2), \tag{3.48}$$

$$\frac{dL}{dt} = v_I - \sigma L(t)^2. \tag{3.49}$$

To numerically approximate equations (3.43) - (3.49), the spatial domain is split into n grid points. The spacing of these points will be referred to as Δz and the time step will be Δt. Superscripts i are used to denote temporal time steps and subscripts j to denote spatial grid points. The equations for the two species are reaction advection equations and a time splitting scheme is used to separate the reaction and advection terms. These two separate parts are then solved using a forward Euler scheme and composed to give us a numerical approximation to the solution. This time splitting scheme is only used to approximate (3.43) and then (3.44) is solved using the assumption that $X_1 + X_2 = 1 - \epsilon_\ell$. The first step in this process is to approximate the velocity. This

is done by integrating equation (3.48) from 0 to z to obtain an integral equation for the velocity.

$$v = L(t) \int_0^z \frac{\mu_2 N}{(k_2 + N)(1 - \epsilon_\ell)} (qX_1 + X_2) ds \tag{3.50}$$

To approximate (3.50), the trapezoid rule is used to create a matrix for integration. This matrix is then applied to the discretized right hand side of equation (3.50) to obtain an approximation of the velocity at each grid point for a fixed time. Define a vector $f := \frac{\mu_2 N}{(k_2+N)(1-\epsilon_\ell)}(qX_1 + X_2)$, then the integration matrix applied to the the vector f looks like the following

$$v = \frac{L(t)\Delta z}{2} \begin{bmatrix} 0 & 0 & 0 & 0 & 0 & 0 \\ 1 & 1 & 0 & 0 & 0 & 0 \\ 1 & 2 & 1 & 0 & 0 & 0 \\ 1 & 2 & 2 & 1 & 0 & 0 \\ 1 & 2 & 2 & 2 & \ddots & 0 \\ 1 & 2 & 2 & \cdots & 2 & 1 \end{bmatrix} \begin{bmatrix} f_1^i \\ f_2^i \\ f_3^i \\ f_4^i \\ \vdots \\ f_n^i \end{bmatrix}.$$

Now that the velocity has been approximated for a fixed time, the time splitting scheme can be implemented to approximate equation (3.43) by splitting the equation into the following two parts

$$\frac{\partial X_1}{\partial t} = \left(\frac{dL(t)}{dt} z - v \right) \frac{\partial X_1}{\partial z} \frac{1}{L(t)}, \tag{3.51}$$

$$\frac{\partial X_1}{\partial t} = \frac{q\mu_2 N}{k_2 + N} X_1 - \frac{\partial v}{\partial z} \frac{X_1}{L(t)}. \tag{3.52}$$

To approximate X_1 in equation (3.51), a second order ENO up winding scheme is implemented to determine an approximation for $\left(\frac{dL(t)}{dt} z - v \right) \frac{\partial X_1}{\partial z} \frac{1}{L(t)}$ [12]. Then equation (3.51) is approximated using the forward Euler method by taking a half of a time step

$$X_{1,j}^{i+\frac{1}{2}} = X_{1,j}^{i} + \Delta t \left[\frac{\partial X_1}{\partial z} \left(\frac{dL(t)}{dt} \frac{z}{L(t)} - \frac{v}{L(t)} \right) \right]_j^i. \tag{3.53}$$

Once a numerical approximation for $X_{1,j}^{i+\frac{1}{2}}$ is obtained, these new values of X_1 are used in (3.52) to obtain a numerical approximation for $X_{1,j}^{i+1}$ by taking another half of a time step for the reaction terms. This is also done with the forward Euler method

$$X_{1,j}^{i+1} = X_{1,j}^{i+\frac{1}{2}} + \Delta t X_{1,j}^{i+\frac{1}{2}} \left[\frac{qmN}{a+N} - \frac{\partial v}{\partial z} \frac{1}{L(t)} \right]_j^i. \tag{3.54}$$

Note that in the code, the right hand side of equation (3.33) is used for the term $\frac{\partial v}{\partial z} \frac{1}{L(t)}$. Since the condition that the volume fractions of the species must add to $1 - \epsilon_\ell$ has been imposed. The volume fraction for X_2 can be found at each spatial grid point by using $X_2 = 1 - X_1 - \epsilon_\ell$. Note that this is just for the model without death terms. If equation (3.42) is included in the model, then the time splitting method would need to be used on equations (3.40) and (3.41). This time though, the death terms would need to be included in the reaction operator (3.52). Once X_1 and X_2 have been approximated, equation (3.39) can be used to approximate X_3.

Next, a method needs to be implemented to solve equations (3.45) - (3.47). To do this, an approximation for the Laplacian is needed. The approximation for the Laplacian is found using the second order centered difference

$$f_j'' \approx \frac{f_{j-1} - 2f_j + f_{j+1}}{(\Delta z)^2}. \tag{3.55}$$

The boundary conditions for the dissolved components also need to be considered. To do this, the second order centered difference approximation to the first derivative is used to estimate the Neumann boundary conditions at $z = 0$. For a general function f, the approximation at a spatial grid point j is

$$f_j' \approx \frac{f_{j+1} - f_{j-1}}{2\Delta z}. \tag{3.56}$$

Since all of the left boundary conditions for the dissolved components are Neumann, the point that lies outside of the domain can be solved for and then input into the approximation for the Laplacian. This calculation yields $f_{-1} = f_1$. For the Dirichlet boundary conditions at $z = 1$, the last row of the matrix that is used to approximate the Laplacian can be set to all $0'$s except for the last entry which is a 1. To implement this, the last entry must be the reciprocal of whatever multiplies the matrix. Putting all of this together, a matrix that approximates the Laplacian at each spatial grid point will look like the following,

$$\frac{1}{(\Delta z)^2}\begin{bmatrix} -2 & 2 & & & & & & \\ 1 & -2 & 1 & & & & & \\ & 1 & -2 & 1 & & & & \\ & & 1 & -2 & 1 & & & \\ & & & \ddots & \ddots & \ddots & & \\ & & & & 1 & -2 & 1 & \\ & & & & & & & (\Delta z)^2 \end{bmatrix}. \tag{3.57}$$

So for example, equation (3.45) would now look like the following for the discretized system

$$D\begin{bmatrix} -2 & 2 & & & & & & \\ 1 & -2 & 1 & & & & & \\ & 1 & -2 & 1 & & & & \\ & & 1 & -2 & 1 & & & \\ & & & \ddots & \ddots & \ddots & & \\ & & & & 1 & -2 & 1 & \\ & & & & & & & \frac{1}{D} \end{bmatrix}\begin{bmatrix} S_1 \\ S_2 \\ S_3 \\ S_4 \\ S_5 \\ \vdots \\ S_n \end{bmatrix} - L^2(\Delta z)^2\begin{bmatrix} G_1(E,S) \\ G_2(E,S) \\ G_3(E,S) \\ G_4(E,S) \\ \vdots \\ G_{n-1}(E,S) \\ 0 \end{bmatrix} + \begin{bmatrix} 0 \\ 0 \\ 0 \\ 0 \\ \vdots \\ 0 \\ -Sb \end{bmatrix} = \begin{bmatrix} 0 \\ 0 \\ 0 \\ 0 \\ \vdots \\ 0 \\ 0 \end{bmatrix},$$

where the last entry of the matrix for $G(E,S)$ is 0 and the Dirichlet boundary condition is

accounted for by adding a vector of all $0's$ and including the boundary condition in the last entry. Note that $(\Delta z)^2$ and $L^2(t)$ have been moved onto the reaction terms.

Implementing Robin conditions for equations (3.45) - (3.47) is not that difficult and only requires a few changes. To numerically approximate equation (3.18), use equation (3.56) and after accounting for the change of variables for the moving boundary, the result will be

$$D\frac{S_{n+1} - S_{n-1}}{2L(t)\Delta z} = \beta(Sb - S_n). \tag{3.58}$$

Then solve for S_{n+1} to get that

$$S_{n+1} = \frac{2L\Delta z\beta}{D}(Sb - S_n) + S_{n-1}. \tag{3.59}$$

Equation (3.59) is then plugged into the second order central difference approximation to obtain the same matrix as in (3.57) except the last row will be different. The matrix will be the following after defining $\alpha := 2\left(\frac{-L\beta\Delta z}{D} - 1\right)$ and $\psi := 2L(t)\Delta z\beta Sb$,

$$\frac{D}{L^2(\Delta z)^2}\begin{bmatrix} -2 & 2 & & & & & & \\ 1 & -2 & 1 & & & & & \\ & 1 & -2 & 1 & & & & \\ & & 1 & -2 & 1 & & & \\ & & & \ddots & \ddots & \ddots & & \\ & & & & 1 & -2 & 1 & \\ & & & & & 2 & \alpha & \end{bmatrix} + \begin{bmatrix} 0 \\ 0 \\ 0 \\ 0 \\ 0 \\ \vdots \\ \psi \end{bmatrix}, \tag{3.60}$$

where the added vector is what is left over from approximating the point S_{n+1}.

This provides an outline on how to discretize equations (3.45) - (3.47) for Robin and Dirichlet boundary conditions. These discretized equations are then solved using, a generalized minimum

residual method established in [9]. Note that the dissolved components are lagging behind in time. This is because equations (3.43) and (3.44) were chosen to be approximated first. The updated values for the two species are used to approximate the solutions for the dissolved components.

Finally an approximation is needed for equation (3.49) which tells us how the thickness $L(t)$ of the biofilm evolves. This is done by taking taking the value of the velocity at $z = 1$ after having approximated equation (3.48) and then using the explicit forward Euler method to approximate the biofilm thickness. The thickness is calculated before the dissolved components are approximated.

Included below is a pseudo code of how the time splitting is implemented. The time t is not actually divided by 2, but instead equation (3.51) is approximated and then those values are used to approximate equation (3.52) in the same loop followed by an approximation for the dissolved components.

```
1: for iter:1:9000
2: advec_step    %compute convection term and update Species
3: react_step    %take a time step for reaction terms using values from advec_step
4: sub_step    % calculate dissolved component value using gmres
5: end
```

Algorithm 3.1: How time splitting is implemented

RESULTS

Numerical Approximations to the biofilm model

In Chapter 2, the chemostat model in [15] was adapted to a biofilm model along with a rigorous framework for numerically solving this new system. Note that the biofilm model developed in Chapter 2 does not apply to a specific species but provides a general framework for how to model competition in a biofilm. The two species are dimensionless volume fractions, while the nutrient, enzyme, and substrate are dimensionless and represent concentrations. The time and spatial dimension are dimensionless as well. The model is intended to give a qualitative idea of what could happen in a biofilm.

The parameters are chosen to be similar to the ones given in [15] to reflect what an adaptation of the chemostat model would be in a biofilm so that the differences between models can be compared. A list of the parameter values can be found in Table 4. The liquid volume fraction ϵ_ℓ is assumed to be negligible and thus is set to 0. This says that the volume taken up by the dissolved components is is not a major factor in the growth of the biofilm. The initial volume fraction of the cooperator is $X_1 = .8$ which forces an initial volume fraction of cheater species $X_2 = .2$. Note that the the parameter μ_1 used in the Monod function $G(E, S)$ was chosen to be 5 for these simulations while $a = 20$ was used in [15] for $G(E, S) = aES$. This would not change the ultimate outcome seen in Figure 2.3 if a had been chosen to be 5 since Theorem 2.0.1 would still apply and the tragedy could still happen.

The first numerical simulation that was run used the Dirichlet boundary conditions for the dissolved components at $z = 1$ and Neumann boundary conditions at $z = 0$ which are outlined in equations (3.15) - (3.17). It is assumed that there is initially some enzyme in the biofilm like in the chemostat model. Note that in Figure 4.1 the values of E, S and N have been scaled by their maximum values so that all the values on the plot lie in $[0, 1]$. This does not change their behavior since they are just being scaled by constants. The substrate has a positive gradient into the biofilm

Table 4.1: Parameter Values Used in Numerical Simulations

Parameter	Description	value
Sb	Substrate bulk concentration	10
E_I	Initial Enzyme concentration	.2
k_1	half saturation concentration for enzyme	.05
k_2	half saturation constant for nutrient	.05
μ_1	maximum growth rate for enzyme	5
μ_2	maximum growth rate for nutrient	5
D	Diffusion coefficient	10
β	Robin condition coefficient	10
γ	yield	1
q	fraction of growth for X_1	.8
ϵ_ℓ	liquid volume fraction	0
σ	Detachment constant	.05

which is achieved by making the substrate value at $z = 1$ larger than the initial concentration of substrate. The nutrient and enzyme are both zero at the boundary since it has been assumed that there is no enzyme or nutrient in the bulk liquid phase. The biofilm thickness $L(t)$, grows at a rapid rate at first and then levels out for the rest of the simulation. This would seem to suggest a steady state, which is explored in depth in Chapter 5. The results in Figure 4.1 are qualitatively different from those seen in Figures 2.3 and 2.4. The results suggest that cooperation between X_1 and X_2 is possible in a biofilm as opposed to a chemostat and a tragedy of the commons can be avoided when a spatial element is introduced.

The next numerical experiment that was conducted included all the same parameter values, except now the Robin boundary conditions are implemented at the right boundary by using

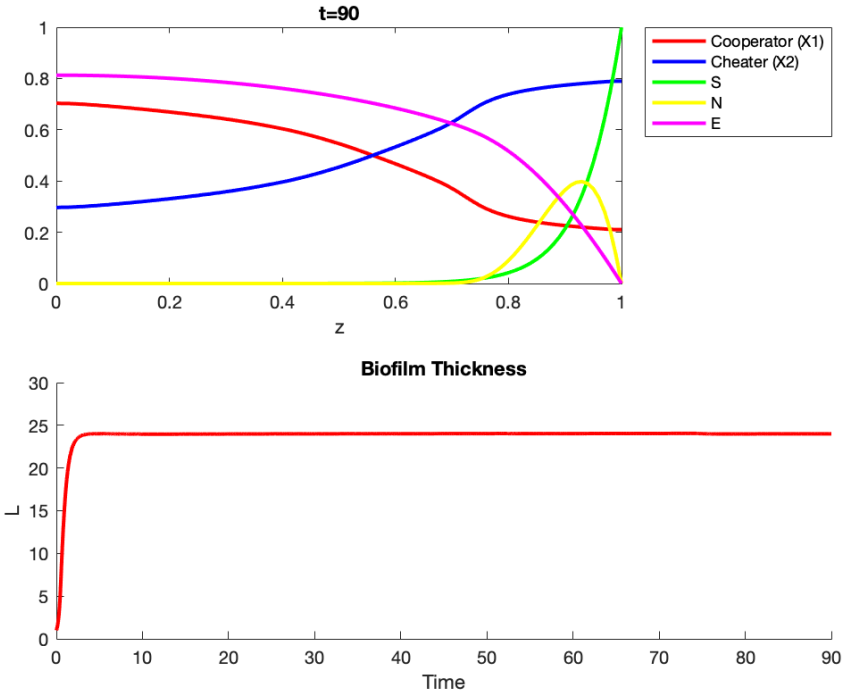

Figure 4.1: Numerical Simulation with parameter values from Table 4 found with a spacial grid of 101 points and grid spacing $\Delta z = .01$ and a time step of $\Delta t = .01$ under Dirichlet boundary conditions. Note that S, E, and N are scaled by their maximum values. The results indicate that a tragedy of the commons is avoided. Time was allowed to run until $t = 90$. The top image is a graph of the indicated components as a function of z at $t = 90$ and seems to be a steady state of the system. The bottom graph is shows the biofilm thickness as a function of time.

equations (3.18) - (3.20). The left boundary is still Neumann like the numerical experiment in Figure 4.1. Qualitatively, the results in Figure 4.2 are similar to those found in the numerical experiment for the Dirichlet boundary conditions at $z = 1$. There appears to be no major differences in the volume fractions of the two species. This is to be expected since the Dirichlet boundary conditions can be recovered from the Robin boundary conditions if $\beta \to \infty$.

One difference to note, is that the biofilm thickness is slightly less than the thickness attained with the Dirichlet conditions. This is most likely because the maximum substrate concentration obtained when using the Robin conditions is less than when using the Dirichlet conditions. The right boundary for both the nutrient and enzyme is now also different. It can be seen in Figure 4.2

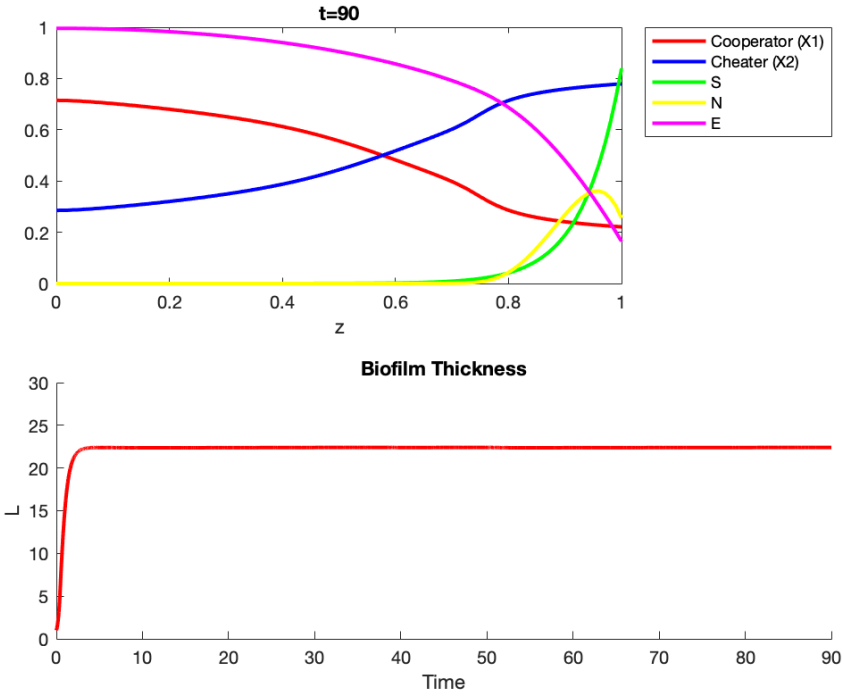

Figure 4.2: Numerical Simulation with parameter values from Table 4 found with a spacial grid of 101 points and grid spacing $\Delta z = .01$ and a time step of $\Delta t = .005$ under Robin boundary conditions. Note that S, E, and N are scaled by their maximum values. The time simulation was run until $t = 90$. The top image is a graph of the indicated components as a function of z at $t = 90$ and seems to be a steady state of the system. The results indicate that a tragedy of the commons is avoided. The bottom graph is shows the biofilm thickness as a function of time.

that both the enzyme and nutrient have a negative gradient at the right boundary $z = 1$ and their values are no longer 0 at this boundary. This indicates that the enzyme and nutrient are leaking out into the bulk liquid while the substrate still has a positive gradient at the boundary and is coming into the biofilm. The only difference in running this numerical experiment compared with the Dirichlet conditions is that a smaller time step was taken. The Robin conditions are considered since they mathematically model liquid moving over the top of the biofilm. This is different than the Dirichlet conditions which model stagnant water at the biofilm bulk liquid interface. Ultimately, similar qualitative results are achieved no matter if Dirichlet or Robin conditions are used at $z = 1$.

The results seen in Figures 4.1 and 4.2 indicate that a tragedy of the commons is avoided. It appears as if the cooperator and cheater can exist together without going extinct. This result is significant because under similar conditions in a chemostat, both species go extinct. These results have to be interpreted carefully though. The results in Figures 4.1 and 4.2 do not definitively prove that this is the long term stable steady-state of the system since time was only allowed to run until $t = 90$.

These results provide something different to what is seen in the biofilm model in [10]. Recall that in [10] the two species had different growth rates, one of the species performed better at higher substrate concentrations and the other at low substrate concentrations. In [10], it was shown that two species competing for a single limiting substrate would lead to the exclusion of one of the species depending on the amount of substrate available. The results in this thesis seem to demonstrate that cooperation is possible and that neither of the species is excluded. The model in this thesis considers a more complex interaction between dissolved components to produce nutrient, which is different than the single nutrient used in [10]. Note that in [10], it was shown that cooperation was possible between two species if the species were allowed to diffuse downward in the biofilm. This thesis has demonstrated a possible circumstance in which cooperation between two competing species is possible without downward diffusion.

STABILITY ANALYSIS

Steady States and Numerical Perturbations

The results found in Figures 4.1 and 4.2 seem to suggest that this system eventually goes to a steady state for both Robin and Dirichlet conditions at the boundary $z = 1$. Now some numerical methods will be used to demonstrate that the results in Figures 4.1 and 4.2 are indeed steady states.

The first approach involves letting time run until the biofilm thickness starts to level out and then solving the system of equations (3.43) - (3.48) to steady state. To do this, the thickness L is assumed to be constant and all the components are assumed to be in steady state, so the system of equations that is being solved is as follows

$$\frac{\partial v}{\partial z}\frac{X_1}{L} + v\frac{\partial X_1}{\partial z}\frac{1}{L} - \frac{q\mu_2 N}{k_2 + N}X_1 = 0, \tag{5.1}$$

$$\frac{\partial v}{\partial z}\frac{X_2}{L} + v\frac{\partial X_2}{\partial z}\frac{1}{L} - \frac{\mu_2 N}{k_2 + N}X_2 = 0, \tag{5.2}$$

$$\frac{D}{L^2}\frac{\partial^2 S}{\partial x^2} - S\frac{\mu_1 E}{k_1 + E} = 0, \tag{5.3}$$

$$\frac{D}{L^2}\frac{\partial^2 E}{\partial x^2} + \frac{(1-q)\mu_2 N}{k_2 + N}X_1 = 0, \tag{5.4}$$

$$\frac{D}{L^2}\frac{\partial^2 N}{\partial x^2} + S\frac{\mu_1 E}{k_1 + E} - \frac{1}{\gamma}(X_1 + X_2)\frac{\mu_2 N}{k_2 + N} = 0, \tag{5.5}$$

$$\frac{\partial v}{\partial z}\frac{1}{L} - \frac{\mu_2 N}{(k_2 + N)(1 - \epsilon_\ell)}(qX_1 + X_2) = 0. \tag{5.6}$$

These equations are then discretized following the example outlined in equation (3.57) and the same generalized minimum residual method that was used to solve for the dissolved components is now used to solve equations (5.1) - (5.6). Note that when these equations are numerically approximated, equation (5.1) is approximated and then the numerical approximation for X_2 can be found by taking $X_2 = 1 - X_1$. When equations (5.1) - (5.6) are approximated, they are indistinguishable from the values for the two species, substrate, enzyme, and nutrient in Figures

4.1 and 4.2. This is a strong indication of the possibility of a steady state.

Another numerical approach can be implemented to see if the biofilm profiles are steady states by perturbing the system by a random amount. First, the time simulation is run until it appears that the system has reached a stable equilibrium. The data is then taken from this simulation and a small ϵ perturbation is added to S, E, N, X_1 and X_2. The perturbations are generated in Matlab by creating random vectors with values in $(0, 1)$. These random values are then scaled by a factor of $.04$ and added to the proposed steady state solution values. So all of the random values added to the proposed steady state are in $[0, .04]$. Note that to perturb X_2, a perturbation need only be added to X_1 and then the perturbed value of X_1 is subtracted from 1 to get the perturbed X_2. This ensures that the volume fractions of X_1 and X_2 still add to 1. The perturbed values that are plugged into the time simulation code read

$$S = S^* + \epsilon_1, \tag{5.7}$$

$$E = E^* + \epsilon_2, \tag{5.8}$$

$$N = N^* + \epsilon_3, \tag{5.9}$$

$$X_1 = X_1^* + \epsilon_4, \tag{5.10}$$

$$X_2 = 1 - X_1^* + \epsilon_4. \tag{5.11}$$

The stars denote the proposed stable steady state values. The ϵ_i for $i = 1, 2, 3, 4$ denote that the perturbations being added and are all different. Once the system is perturbed, the time code is run with the perturbed values to see if the system tends to the proposed steady state values or goes to something else. The results are shown in Figure 5.1. The graph in the bottom of Figure 5.1 shows the perturbed values of the components. The top graph shows what happens after letting time run again with the perturbed values as the initial conditions. This result suggests that a stable steady state has been found since the perturbed initial values return to values that are indistinguishable from the results in Figure 4.1 when time is allowed to run again.

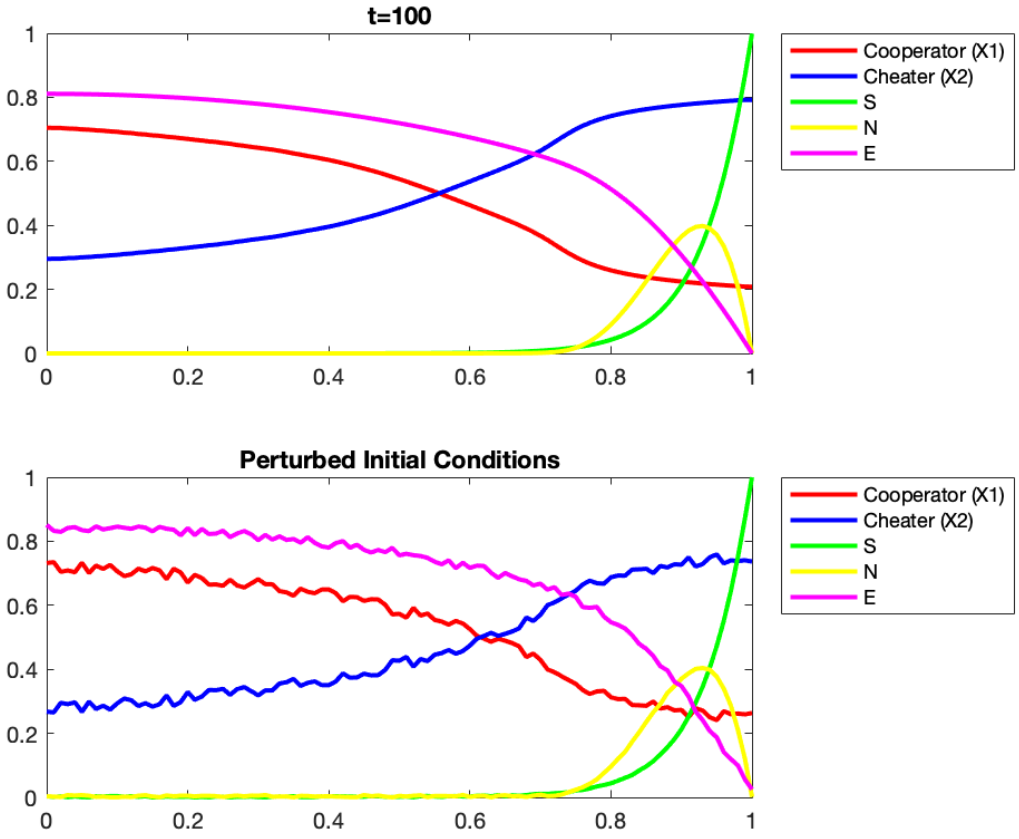

Figure 5.1: The top image is shows the values of X_1, X_2, S, E, and N after perturbing them and then letting them run another 10 time units until $t = 100$ with Dirichlet boundary conditions at $z = 1$. The bottom image is the initial condition with the perturbations added.

A similar result is achieved when the proposed steady-state values from the time simulation with Robin conditions are perturbed. These results can be seen in Figure 5.2. When the perturbed values are used as initial conditions and time is allowed to run again, the perturbed values tend back to the proposed steady state values (see Figure 5.2).

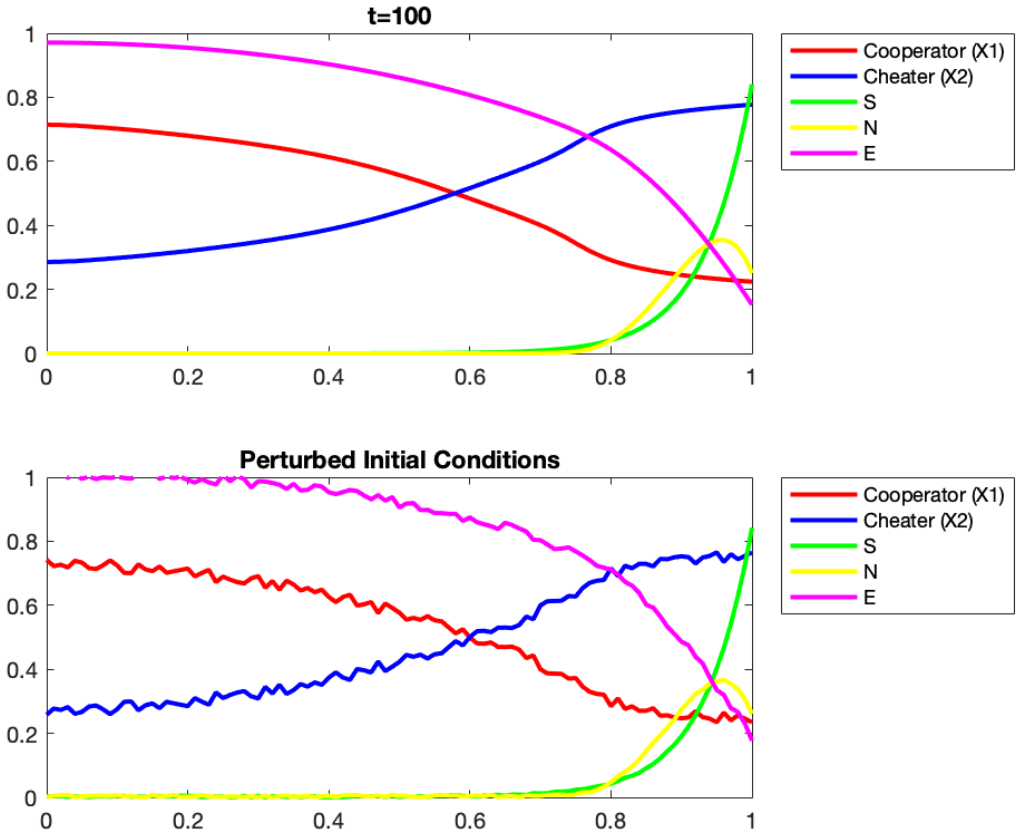

Figure 5.2: The top image is shows the values of X_1, X_2, S, E, and N after perturbing them and then letting time run until for another 10 time units until $t = 100$ with Robin boundary conditions at $z = 1$. The bottom image is the initial condition where the perturbations have been added.

Linearization

While the results of perturbing the system are promising in the search for a stable steady state, they are by no means a proof for its existence. To further convince the reader that the results in Figures 4.1 and 4.2 are actually steady states, another approach is taken. The approach involves linearizing equations (3.43), (3.45), (3.46), (3.47), and (3.33). Once the system is linearized, the eigenvalues of the discretized system are computed. In this process, the biofilm thickness is not perturbed and is assumed to be the constant value achieved in Figure 4.1. The value of X_1 in (3.43)

is perturbed by some amount say ϵ, and this forces the perturbation of X_2 in equation (3.44) to be $-\epsilon$, to ensure that $X_1 + X_2 = 1$. Even though the time derivatives of equations (3.30) - (3.32) were assumed to be negligible, they must be considered here to explain how small perturbations evolve in time. So, the system of equations that needs to be linearized is as follows

$$\frac{\partial X_1}{\partial t} = -\frac{\partial X_1}{\partial z}\frac{1}{L} - X_1\frac{\mu_2 N}{(k_2+N)}(qX_1 + 1 - X_1) + \frac{q\mu_2 N}{k_2+N}X_1, \tag{5.12}$$

$$\frac{\partial S}{\partial t} = \frac{D}{L^2}\frac{\partial^2 S}{\partial x^2} - S\frac{\mu_1 E}{k_1+E}, \tag{5.13}$$

$$\frac{\partial E}{\partial t} = \frac{D}{L^2}\frac{\partial^2 E}{\partial x^2} + \frac{(1-q)\mu_2 N}{k_2+N}X_1, \tag{5.14}$$

$$\frac{\partial N}{\partial t} = \frac{D}{L^2}\frac{\partial^2 N}{\partial x^2} + S\frac{\mu_1 E}{k_1+E} - \frac{1}{\gamma}\frac{\mu_2 N}{k_2+N}, \tag{5.15}$$

$$0 = \frac{\mu_2 N}{(k_2+N)}(qX_1 + 1 - X_1) - \frac{\partial v}{\partial z}\frac{1}{L}. \tag{5.16}$$

In the system (5.12) - (5.16), X_2 was replaced by $1 - X_1$. Also, in equation (5.12), $\frac{\partial v}{\partial z}\frac{1}{L}$ has been replaced by $\frac{\mu_2 N}{(k_2+N)}(qX_1 + 1 - X_1)$. Again, the stars will denote steady state solutions and the hats will denote the perturbed function being added to the proposed steady state. The new functions will read

$$X_1 = X_1^* + \epsilon\hat{X}_1, \tag{5.17}$$

$$S = S^* + \epsilon\hat{S}, \tag{5.18}$$

$$E = E^* + \epsilon\hat{E}, \tag{5.19}$$

$$N = N^* + \epsilon\hat{N}, \tag{5.20}$$

$$v = v^* + \epsilon\hat{v}. \tag{5.21}$$

Now substitute equations (5.17) - (5.21) into equations (5.12) - (5.16). Once this is done, take the derivative with respect to ϵ and evaluate at $\epsilon = 0$ and assume that any term multiplied by ϵ^2 is small

enough to be negligible. The system of linear equations will then be

$$\frac{\partial \hat{S}}{\partial t} = \frac{D}{L^2}\frac{\partial^2 \hat{S}}{\partial z^2} - \frac{\mu_1 E^*}{k_1 + E^*}\hat{S} - S^*\frac{\mu_1 k_1}{(k_1+E)^2}\hat{E}, \tag{5.22}$$

$$\frac{\partial \hat{E}}{\partial t} = \frac{D}{L^2}\frac{\partial^2 \hat{E}}{\partial z^2} + (1-q)\left[\frac{\mu_2 N^*}{k_2+N^*}\hat{X}_1 + X_1^*\frac{\mu_2 k_2}{(k+N^*)^2}\hat{N}\right], \tag{5.23}$$

$$\begin{aligned}\frac{\partial \hat{N}}{\partial t} = &\frac{D}{L^2}\frac{\partial^2 \hat{N}}{\partial z^2} + \frac{\mu_1 E^*}{k_1+E^*}\hat{S} + S^*\frac{\mu_1 k_1}{(k_1+E)^2}\hat{E} \\ &- \frac{1}{\gamma}\left[\frac{\mu_2 k_2}{(k+N^*)^2}\hat{N}\right]\end{aligned}, \tag{5.24}$$

$$\begin{aligned}\frac{\partial \hat{X}_1}{\partial t} = &(q-1)\frac{\mu_2 N^*}{k_2+N^*}\hat{X}_1 - 2(q-1)X_1^*\frac{\mu_2 N^*}{k_2+N^*}\hat{X}_1 - \frac{1}{L}\left[\frac{\partial \hat{X}_1}{\partial z}v^* + \frac{\partial X_1^*}{\partial z}\hat{v}\right], \\ &+ \left[(q-1)(X_1^* - X_1^{*^2})\right]\frac{\mu_2 k_2}{(k+N^*)^2}\hat{N}\end{aligned} \tag{5.25}$$

$$0 = -\frac{\partial \hat{v}}{\partial z}\frac{1}{L} + \left[(q-1)\frac{\mu_2 N^*}{k_2+N^*}\hat{X}_1 + (qX_1^* + 1 - X_1^*)\frac{\mu_2 k_2}{(k+N^*)^2}\hat{N}\right]. \tag{5.26}$$

The set of equations (5.22) - (5.26) are now linear in $\hat{X}_1$, $\hat{S}$, $\hat{E}$, $\hat{N}$, and $\hat{v}$. Since the original set of equations (3.43) - (3.49) were solved numerically, equations (5.22) - (5.26) will be discrete as well. So a matrix A will be created to describe the linear operators associated to each part of the right hand side of equations (5.22) - (5.26). The matrix A will thus be a block matrix. Let $A_{i,j}$ be the blocks of the matrix A that correspond to the linear parts of the discretized right hand side of equations (5.22) - (5.26), then the system will in general look like

$$\begin{bmatrix} \frac{\partial \hat{S}}{\partial t} \\ \frac{\partial \hat{E}}{\partial t} \\ \frac{\partial \hat{N}}{\partial t} \\ \frac{\partial \hat{X}_1}{\partial t} \\ 0 \end{bmatrix} = \left[\begin{array}{c|c|c|c|c} A_{1,1} & A_{1,2} & A_{1,3} & A_{1,4} & A_{1,5} \\ \hline A_{2,1} & A_{2,2} & A_{2,3} & A_{2,4} & A_{2,5} \\ \hline A_{3,1} & A_{3,2} & A_{3,3} & A_{3,4} & A_{3,5} \\ \hline A_{4,1} & A_{4,2} & A_{4,3} & A_{4,4} & A_{4,5} \\ \hline A_{5,1} & A_{5,2} & A_{5,3} & A_{5,4} & A_{5,5} \end{array}\right] \begin{bmatrix} \hat{S} \\ \hat{E} \\ \hat{N} \\ \hat{X}_1 \\ \hat{v} \end{bmatrix}. \tag{5.27}$$

Where $\frac{\partial \hat{S}}{\partial t}$, $\frac{\partial \hat{E}}{\partial t}$, $\frac{\partial \hat{N}}{\partial t}$, $\frac{\partial \hat{X}_1}{\partial t}$, and 0 are all vectors and so are $\hat{S}$, $\hat{E}$, $\hat{N}$, $\hat{X}_1$, and $\hat{v}$. The boundary

conditions must also be linearized and will now read

$$\left.\frac{\partial \hat{S}}{\partial z}\right|_0 = 0 \qquad \hat{S}(1,t) = 0, \tag{5.28}$$

$$\left.\frac{\partial \hat{E}}{\partial z}\right|_0 = 0 \qquad \hat{E}(1,t) = 0, \tag{5.29}$$

$$\left.\frac{\partial \hat{N}}{\partial z}\right|_0 = 0 \qquad \hat{N}(1,t) = 0. \tag{5.30}$$

The matrix A is what needs to be constructed so that its eigenvalues can be computed. An outline of how to compute some of the blocks $A_{i,j}$ follows.

First consider the right hand side of equation (5.22) for the substrate

$$\frac{D}{L(t)^2}\frac{\partial^2 \hat{S}}{\partial z^2} - \frac{\mu_1 E^*}{k_1 + E^*}\hat{S} - S^* \frac{\mu_1 k_1}{(k_1 + E^*)^2}\hat{E}. \tag{5.31}$$

The diffusion operation is the same as in equation (3.57), except the last row is eliminated because the Dirichlet boundary condition at $z = 1$ is $\hat{S}(1,t) = 0$. Now in general the spatial grid consists of n points, so $-\frac{\mu_1 E^*}{k_1+E^*}$ is a vector with n entries. Let $\alpha_i = -\left.\frac{\mu_1 E^*}{k_1+E^*}\right|_i$, where the subscripts denote evaluation at a grid point i. Only $(n-1)$ entries are needed for the vector α, since the Dirichlet boundary condition is $\hat{S}(1,t) = 0$. Thus the matrix that multiplies the vector $\hat{S}$ for the substrate equation will be

$$A_{1,1} = \frac{D}{L^2(\Delta z)^2}\begin{bmatrix} -2 & 2 & & & & & \\ 1 & -2 & 1 & & & & \\ & 1 & -2 & 1 & & & \\ & & 1 & -2 & 1 & & \\ & & & \ddots & \ddots & \ddots & \\ & & & & 1 & -2 & 1 \end{bmatrix} + \begin{bmatrix} \alpha_1 & & & & & & \\ & \alpha_2 & & & & & \\ & & \alpha_3 & & & & \\ & & & \alpha_4 & & & \\ & & & & \ddots & & \\ & & & & & & \alpha_{n-1} \end{bmatrix}. \tag{5.32}$$

Now define $\beta_i := S^* \frac{\mu_1 k_1}{(k_1+E^*)^2}\Big|_i$, then the matrix that multiples the vector $\hat{E}$ will be

$$A_{1,2} = \begin{bmatrix} \beta_1 & & & & & \\ & \beta_2 & & & & \\ & & \beta_3 & & & \\ & & & \beta_4 & & \\ & & & & \ddots & \\ & & & & & \beta_{n-1} \end{bmatrix}. \tag{5.33}$$

Since there are no linear parts involving $\hat{X}_1$, $\hat{N}$, or $\hat{v}$, the matrices that multiply these vectors are all $0'$s. The size of the matrix that multiplies $\hat{N}$ is $n-1 \times n-1$ and the size of the matrices that multiply $\hat{X}_1$ and $\hat{v}$ are $n-1 \times n$. The blocks for equations (5.23) and (5.24) are built the same way as the substrate equation.

Next consider the right hand side of equation (5.25) for the cooperator species

$$\begin{aligned} &(q-1)\frac{\mu_2 N^*}{k_2+N^*}\hat{X}_1 - 2(q-1)X_1^*\frac{\mu_2 N^*}{k_2+N^*}\hat{X}_1 - \frac{1}{L}\left[\frac{\partial \hat{X}_1}{\partial z}v^* + \frac{\partial X_1^*}{\partial z}\hat{v}\right] \\ &+ \left[(q-1)(X_1^* - {X_1^*}^2)\right]\frac{\mu_2 k_2}{(k+N^*)^2}\hat{N} \end{aligned} \tag{5.34}$$

The first thing that is needed is a matrix that approximates the first derivative. The matrix that is implemented uses the first order backwards approximation. This matrix is then multiplied by the values in the vector v^*. Then define $\kappa_i := \left[(q-1)\frac{\mu_2 N^*}{k_2+N^*} - 2(q-1)X_1^*\frac{\mu_2 N^*}{k_2+N^*}\right]\Big|_i$ to be a vector

evaluated at each grid point, and thus the matrix that multiplies $\hat{X}_1$ will be

$$A_{4,4} = -\frac{1}{\Delta z L}\begin{bmatrix} v_1 & & & & & & \\ -v_2 & v_2 & & & & & \\ & -v_3 & v_3 & & & & \\ & & -v_4 & v_4 & & & \\ & & & \ddots & \ddots & & \\ & & & & -v_n & v_n \end{bmatrix} + \begin{bmatrix} \kappa_1 & & & & & & \\ & \kappa_2 & & & & & \\ & & \kappa_3 & & & & \\ & & & \kappa_4 & & & \\ & & & & \ddots & & \\ & & & & & & \kappa_n \end{bmatrix}. \tag{5.35}$$

To get the matrix that multiplies $\hat{v}$, the first order backwards difference approximation is applied to X_1^* which will return a vector that will be called η

$$\eta = -\frac{1}{\Delta z L}\begin{bmatrix} 1 & & & & & & \\ -1 & 1 & & & & & \\ & -1 & 1 & & & & \\ & & -1 & 1 & & & \\ & & & \ddots & \ddots & & \\ & & & & -1 & 1 \end{bmatrix}\begin{bmatrix} X_{1,1}^* \\ X_{1,2}^* \\ X_{1,3}^* \\ X_{1,4}^* \\ \vdots \\ X_{1,n}^* \end{bmatrix}. \tag{5.36}$$

The vector η is then turned into a diagonal matrix that will multiply the vector $\hat{v}$

$$A_{4,5} = \begin{bmatrix} \eta_1 & & & & & \\ & \eta_2 & & & & \\ & & \eta_3 & & & \\ & & & \eta_4 & & \\ & & & & \ddots & \\ & & & & & \eta_n \end{bmatrix}. \tag{5.37}$$

The linear part of the species 1 equation corresponding to $\hat{N}$ is created by making a diagonal matrix out of the vector that multiples it like was done with the substrate equation except that it is size $n \times n-1$ since the Dirichlet boundary condition is $\hat{N}(1,t) = 0$. The matrices that multiply the vector $\hat{S}$ and $\hat{E}$ are all $0'$s of size $n \times n-1$ for the species 1 equation.

Finally, the blocks need to be built for the right hand side of equation (5.26)

$$-\frac{\partial \hat{v}}{\partial z}\frac{1}{L} + \left[(q-1)\frac{\mu_2 N^*}{k_2+N^*}\hat{X_1} + (qX_1^* + 1 - X_1^*)\frac{\mu_2 k_2}{(k+N^*)^2}\hat{N}\right]. \tag{5.38}$$

Again, the first order backwards difference approximation is used to approximate the derivative of $\hat{v}$. So the block that multiplies $\hat{v}$ looks like

$$A_{5,5} = \frac{1}{\Delta z L(t)}\begin{bmatrix} 1 & & & & & & \\ -1 & 1 & & & & & \\ & -1 & 1 & & & & \\ & & & -1 & 1 & & \\ & & & & \ddots & \ddots & \\ & & & & & -1 & 1 \end{bmatrix}. \tag{5.39}$$

Then define the vectors ζ and ω such that $\zeta_i := -(q-1)\frac{\mu_2 N^*}{k_2+N^*}\Big|_i$ and $\omega_i := -(qX_1^* + 1 - X_1^*)\frac{\mu_2 k_2}{(k+N^*)^2}\Big|_i$, where the subscripts just indicate what grid point the functions are being evaluated

at. Thus the blocks that multiply $\hat{X}_1$ and $\hat{N}$ will be

$$A_{5,4} = \begin{bmatrix} \zeta_1 & & & & & \\ & \zeta_2 & & & & \\ & & \zeta_3 & & & \\ & & & \zeta_4 & & \\ & & & & \ddots & \\ & & & & & \zeta_n \end{bmatrix} \tag{5.40}$$

and

$$A_{5,3} = \begin{bmatrix} \omega_1 & & & & & \\ & \omega_2 & & & & \\ & & \omega_3 & & & \\ & & & \ddots & & \\ & & & & & \omega_{n-1} \\ 0 & 0 & 0 & \cdots & 0 & \end{bmatrix}. \tag{5.41}$$

The matrices that multiply $\hat{S}$ and $\hat{E}$ are all $0'$s and are size $n \times n-1$.

Finally, the eigenvalues of the matrix A can be computed. This is done using using the built in eigs algorithm in Matlab [13]. In the code, 60 eigenvalues are computed with real parts closest to $\frac{1}{2}$. Of the 60 eigenvalues computed, only three had positive real part. Two of the eigenvalues computed with positive real part were a complex conjugate pair. The largest real part for the eigenvalues was 3.1409×10^{-5}. This is rather small and could indicate a couple of things. First, it is noted that the three eigenvalues with positive real part could be negative, but due to numerical error, they came out positive. If this is the case, then all the real parts of the eigenvalues computed would be negative and this would be a good indication that the biofilm profile seen in Figure 4.1 is a stable steady state. Second, the eigenvalues could actually be positive, but since they are really small, the perturbation added to the system could grow slowly. This would mean that the results

seen in Figure 4.1 are not actually stable equilibrium values. The disturbances would move slowly with the largest real part of the eigenvalue of 3.1409×10^{-5}. A plot of the 60 computed eigenvalues can be seen in Figure 5.3.

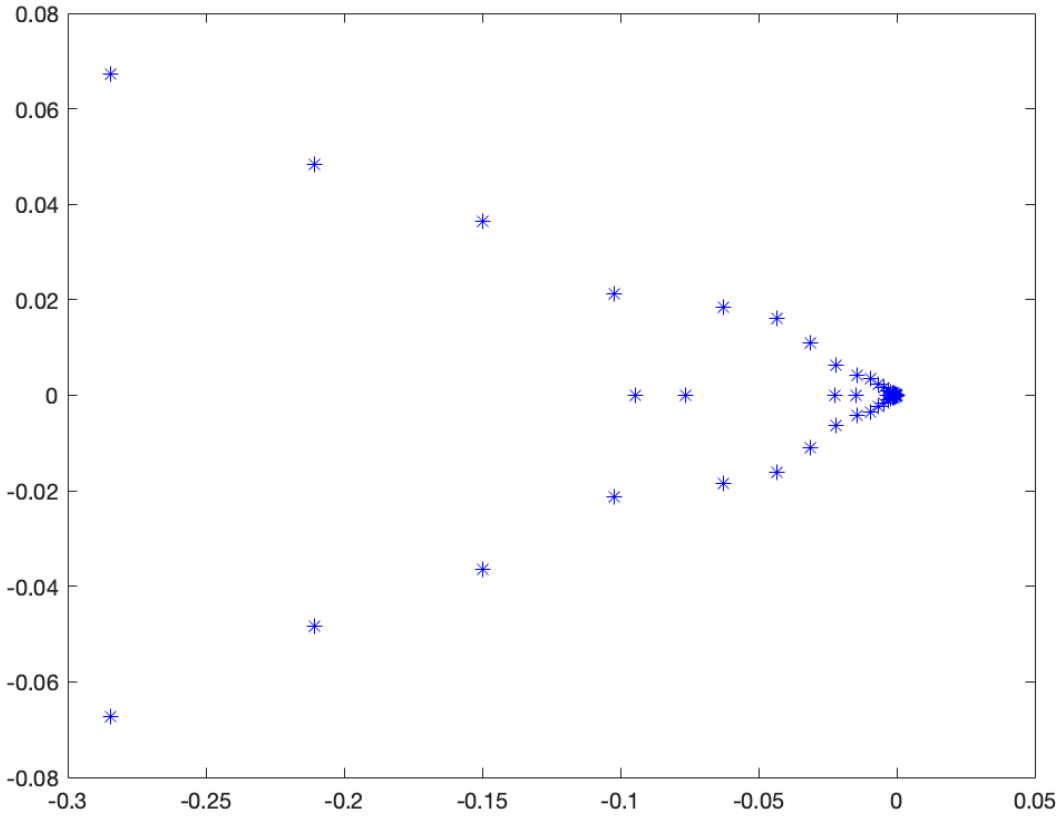

Figure 5.3: The 60 eigenvalues with real part closest to $\frac{1}{2}$ from the matrix A that corresponds to the linear parts of the right hand side of equations (5.22) - (5.26). The eigenvalues are plotted in the complex plane. The constant value of L that was used was $L = 23.9788$

CONCLUSION

This thesis has developed a model in which it appears that cooperation is possible between multiple species. This is by no means a model that describes all the complex interactions within a biofilm. Instead, this model is intended to give a framework for how competition could be modeled within a biofilm. The parameter q that qualitatively describes the competition is not an experimentally determined parameter. The model could be used to test what might happen between different species if specific parameters are chosen. Numerical experiments could then be run with different values of q to get some qualitative information about what may happen in an actual biofilm.

The parameter q that induces competition in the model is a mathematical constant that could prove hard to derive. There are many factors that can impose a burden on a species that puts it at a disadvantage to other species within a biofilm. For instance, in Chapter 1, an example of QS induced competition is given [14] . When wild type PA that requires quorum sensing for growth, is grown with a mutant strain of PA that is quorum sensing deficient, the mutant is shown to have a growth advantage compared to the wild type. Another example of competition in biofilms occurs in PF bacteria when grown in culture tubes. There are two main phenotypes that develop in the culture tube. One of the species called the smooth morphs (SM) lives in the liquid phase of the biofilm while the other species called the wrinkly spreader (WS) forms a biofilm at the liquid air interface. It was demonstrated that the SM type could invade the WS biofilm and lead to the collapse of the the WS biofilm [21]. Then finally in [11], it has been shown that a strain of PA that produces pyoverdine mixed with one that does not can lead to cooperation between two species in a biofilm. In [11], the iron scavenged by pyoverdine can be used by both species. This is perhaps the most similar example to what has been modeled in this thesis and a model for this type of competition can be seen in [4], except in this model, only one species can use the iron scavenged by pyoverdine. These examples give a small sample of how various factors can influence competition in a biofilm

and how challenging it can be to determine the most important aspects of competition.

While it may be hard to determine the main factors of competition in biology, the model presented in this thesis, that has been adapted from a chemostat model in [15], provides some idea of what could happen in biofilms. The results in this thesis for the biofilm model may not apply to a real world species, but they do provide a qualitatively different result from what is seen to happen mathematically for a chemostat model. The model provides a framework for how cooperation can be achieved. In the chemostat model, it is proven for carefully chosen functions and parameters, that a tragedy of the commons is inevitable when a cheater species is mixed with a cooperator. The biofilm model gives a good indication that a tragedy does not occur and that both species can actually coexist at a stable equilibrium. The results in this thesis are also different from what is seen in [10] and [4]. Both of these biofilm models show that competition between two species leads to the exclusion of one species. The main result in this thesis is a model for cooperation between cheaters and cooperators in a biofilm. It has also been argued that the results seen in Figures 4.1 and 4.2 could be stable equilibrium, which would mean that a tragedy is avoided.

REFERENCES CITED

[1] Kyle L Asfahl, Jessica Walsh, Kerrigan Gilbert, and Martin Schuster. Non-social adaptation defers a tragedy of the commons in pseudomonas aeruginosa quorum sensing. *The ISME journal*, 9(8):1734–1746, 2015.

[2] William G. Characklis and Kevin C. Marshall. *Biofilms*. Wiley Series in ecological and applied microbiology. Wiley, New York, NY, 1990.

[3] Rodney M Donlan and J William Costerton. Biofilms: survival mechanisms of clinically relevant microorganisms. *Clinical microbiology reviews*, 15(2):167–193, 2002.

[4] Hermann J Eberl and Shannon Collinson. A modeling and simulation study of siderophore mediated antagonism in dual-species biofilms. *Theoretical Biology and Medical Modelling*, 6(1):1–16, 2009.

[5] Francesca Fiegna, N Yu Yuen-Tsu, Supriya V Kadam, and Gregory J Velicer. Evolution of an obligate social cheater to a superior cooperator. *Nature*, 441(7091):310–314, 2006.

[6] Kevin R Foster, Gad Shaulsky, Joan E Strassmann, David C Queller, and Chris RL Thompson. Pleiotropy as a mechanism to stabilize cooperation. *Nature*, 431(7009):693–696, 2004.

[7] Garrett Hardin. The tragedy of the commons. *science*, 162(3859):1243–1248, 1968.

[8] Sze-Bi Hsu, S Hubbell, and Paul Waltman. A mathematical theory for single-nutrient competition in continuous cultures of micro-organisms. *SIAM Journal on Applied Mathematics*, 32(2):366–383, 1977.

[9] Carl T Kelley. *Iterative methods for linear and nonlinear equations*. SIAM, 1995.

[10] Isaac Klapper and Barbara Szomolay. An exclusion principle and the importance of mobility for a class of biofilm models. *Bulletin of mathematical biology*, 73(9):2213–2230, 2011.

[11] Rolf Kümmerli, Lorenzo A Santorelli, Elisa T Granato, Zoé Dumas, Akos Dobay, Ashleigh S Griffin, and Stuart A West. Co-evolutionary dynamics between public good producers and cheats in the bacterium pseudomonas aeruginosa. *Journal of evolutionary biology*, 28(12):2264–2274, 2015.

[12] Randall J LeVeque et al. *Finite volume methods for hyperbolic problems*, volume 31. Cambridge university press, 2002.

[13] The Mathworks, Inc., Natick, Massachusetts. *MATLAB version 9.1.0.441655 (R2016b)*, 2017.

[14] Kelsi M Sandoz, Shelby M Mitzimberg, and Martin Schuster. Social cheating in pseudomonas aeruginosa quorum sensing. *Proceedings of the National Academy of Sciences*, 104(40):15876–15881, 2007.

[15] Martin Schuster, Eric Foxall, David Finch, Hal Smith, and Patrick De Leenheer. Tragedy of the commons in the chemostat. *PloS one*, 12(12), 2017.

[16] Hal L Smith and Paul Waltman. *The theory of the chemostat: dynamics of microbial competition*, volume 13. Cambridge university press, 1995.

[17] Philip S Stewart. A model of biofilm detachment. *Biotechnology and bioengineering*, 41(1):111–117, 1993.

[18] Philip S Stewart, Brent M Peyton, William J Drury, and Ricardo Murga. Quantitative observations of heterogeneities in pseudomonas aeruginosa biofilms. *Appl. Environ. Microbiol.*, 59(1):327–329, 1993.

[19] Adrien Vigneron, Ian M Head, and Nicolas Tsesmetzis. Damage to offshore production facilities by corrosive microbial biofilms. *Applied microbiology and biotechnology*, 102(6):2525–2533, 2018.

[20] Oskar Wanner and Willi Gujer. A multispecies biofilm model. *Biotechnology and bioengineering*, 28(3):314–328, 1986.

[21] Quan-Guo Zhang, Angus Buckling, Richard J Ellis, and H Charles J Godfray. Coevolution between cooperators and cheats in a microbial system. *Evolution: International Journal of Organic Evolution*, 63(9):2248–2256, 2009.